1996 0118 048

FULL LYAPUNOV EXPONENT PLACEMENT
IN REENTRY TRAJECTORIES

THESIS

Michael H. Platt, Captain, USAF

AFIT/GA/ENY/95D-03

DEPARTMENT OF THE AIR FORCE

AIR UNIVERSITY

AIR FORCE INSTITUTE OF TECHNOLOGY

DTIC QUALITY INSPECTED 3

Wright-Patterson Air Force Base, Ohio

FULL LYAPUNOV EXPONENT PLACEMENT IN REENTRY TRAJECTORIES

THESIS

Presented to the Faculty of the School of Engineering

of the Air Force Institute of Technology

Air University

In Partial Fulfillment of the

Requirements for the Degree of

Master of Science in Astronautical Engineering

Michael H. Platt, B.S., M.B.A.
Captain, USAF

December 1995

Approved for public release; distribution unlimited

Acknowledgments

I would like to thank my advisor, Dr. William Wiesel, Ph.D., for his time, patience and support. His knowledge, expertise, and humor made this a much more bearable experience. I would also like to thank my fellow Astro students, Jay Landis, Dave Parrish, and Greg Schultz for their help with all the little problems that cropped up during this process. I would like to express my gratitude to my parents for making me believe that this was possible. And finally, I wish to thank my wife, Auline, for the great editing job on this thesis. Any errors are mine, not hers. I also offer my thanks to her for putting up with all my bad moods and long nights throughout the whole AFIT program.

Table of Contents

List of Figures

List of Tables

List of Symbols

A   aerodynamic vector containing Lift and Drag forces
α angle of attack
b   atmospheric constant 3.3139×10^{-7} (1/m)
χ cone half angle
C   weighting matrix that discourages deviations from the nominal trajectory
D   drag
D   weighting matrix that discourages the use of control
e   displacement
ϕ latitude
F   force vector
Φ state transition matrix
γ flight path angle
g   acceleration vector due to gravity
G   gain matrix
J   linear quadratic regulator cost function
L   lift
L   Lyapunov exponent
λ Lagrange multiplier
$\mathbf{L_{Zi}}$ lapse rate
m   mass
n   normal vector
P   pressure
θ longitude
r   radius
R   gas constant for air
ρ density of air
σ roll
S   base area of the reentry vehicle
$\mathbf{S_f}$ weighting matrix that discourages deviations from the nominal trajectory final conditions
T   thrust
T   temperature
t   time
u   state space control vector
v   speed
V   volume
ω angular velocity
x   state space state vector
ψ heading
ζ angle between the projection of the normal vector on the b_2, b_3 plane and the b_2 axis (see Appendix A)
Z   altitude

AFIT/GA/ENY/95D-03

Abstract

This study investigated the ability to control the chaotic reentry of a Delta Clipper-like vehicle by setting the values of the initial and final principal dynamical directions as well as the Lyapunov exponents. A model of the original controlled reentry vehicle was created through the use of the equations of motion in conjunction with an atmospheric model. A modified linear quadratic regulator allowed the set up of a boundary value problem which specified the Lyapunov exponents and determined the gain matrix as a function of time. The gain matrix can eventually be used in the control system of the vehicle.

FULL LYAPUNOV EXPONENT PLACEMENT

IN REENTRY TRAJECTORIES

I. INTRODUCTION

1.1 Overview   The goal of this paper is to apply the algorithm developed by Wiesel [13]

for specifying Lyapunov exponents, as well as initial and final principal dynamical

directions in a controlled chaotic system. The algorithm makes use of a modified linear

quadratic regulator to set up a boundary value problem. When solved, this yields the

specified Lyapunov exponents (which describe the stability of the system), the initial and

final dynamical directions and the gain matrix over a specified period of time. The gain

matrix can then be used in the control system of the reentry vehicle. The real world system

used to apply this methodology is a Delta Clipper-like launch vehicle. In the second

chapter of this paper, we discuss the development of the dynamics model of the vehicle

reentry trajectory. The third chapter develops the control algorithm. We then detail the

computer code used to implement the model and control algorithm in Chapter 4. Chapter

5 evaluates the results obtained when we attempt to stabilize the chaotic reentry trajectory

of the vehicle model. Finally, Chapter 6 contains conclusions drawn from the results of

this research and recommendations for further study.

1.2 Vehicle Background   The Delta Clipper Experimental Launch Vehicle (DCX) was

a Single Stage To Orbit (SSTO), Vertical Take-off, Vertical Landing (VTVL) vehicle

developed by the McDonnell Douglas Corporation under the guidance of the Air Force's

Ballistic Missile Defense Organization (BMDO). This was the first in a series of planned

advanced technology demonstration programs whose eventual goal was to develop

operational SSTO systems. It was hoped that, when fully developed, these systems would

significantly lower the cost per pound to orbit of the U.S. space fleet. The BMDO

designed, fabricated, and flight tested the Delta Clipper vehicle in less than 2 years for

under $70 million. Since then, the BMDO has been directed to deal only with ground-

based missile defense, effectively halting their research in the area of SSTO technology

upon completion of the DCX test program. Currently, the SSTO program is under the

control of NASA, which continues to develop two separate SSTO systems, the X-33 and

the   X-34. Of the two vehicles, the X-33 is more likely to resemble the Delta Clipper in

operation and appearance.

A 15 month NASA Concept Definition and Design Phase, initiated in April 1995,

solicited industry teams to compete for the contract to build the X-33. There are three

contractor teams currently involved in this phase. Since the McDonnell Douglas design is

the only one following the VTVL philosophy, we will be using a design similar to theirs

for this project. The final specifications of this version of the X-33 have yet to be

determined, so we will use variations on one of the several proposed designs, seen in

Figure 1-1, as a model for this research.

The main goal of the Delta Clipper program was to create aircraft-like operations

within the space community. The current X-33 vehicle design uses liquid oxygen and

hydrogen for its main engines, and gaseous oxygen and hydrogen for its reaction control

engines. The on-board adaptive guidance will allow the vehicle to handle winds during both launch and landing. During the ascent to orbit, the 8 main engines provide axial acceleration and lateral control. Upon reentry, the aerodynamic controls are used to affect the orientation of the vehicle The pre-landing rotation maneuver covers the angle of attack range of 10° to 180°. The control of this rotation is handled by gimballing the main engines.

Vertical Height: 127 ft
Base Width 18 ft
Empty Weight: 104,100 lb
3 main engines
5 Maneuevering Engines

127 ft

18 ft
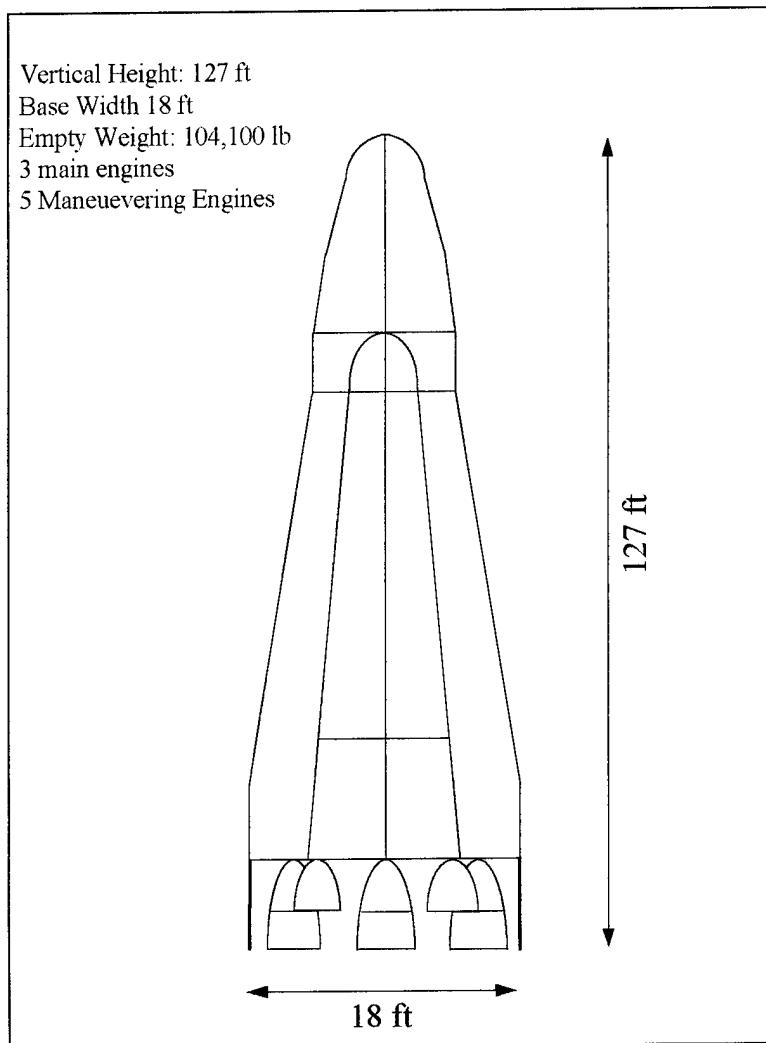
Figure 1-1 X-33 Proposed Design Alternative

Figure 1-2 illustrates a typical launch as well as a rotation maneuver. In standard operations, the rotation maneuver occurs at the end of the trajectories discussed in this study.

Reentry/Landing

Launch to Orbit

Pitchover
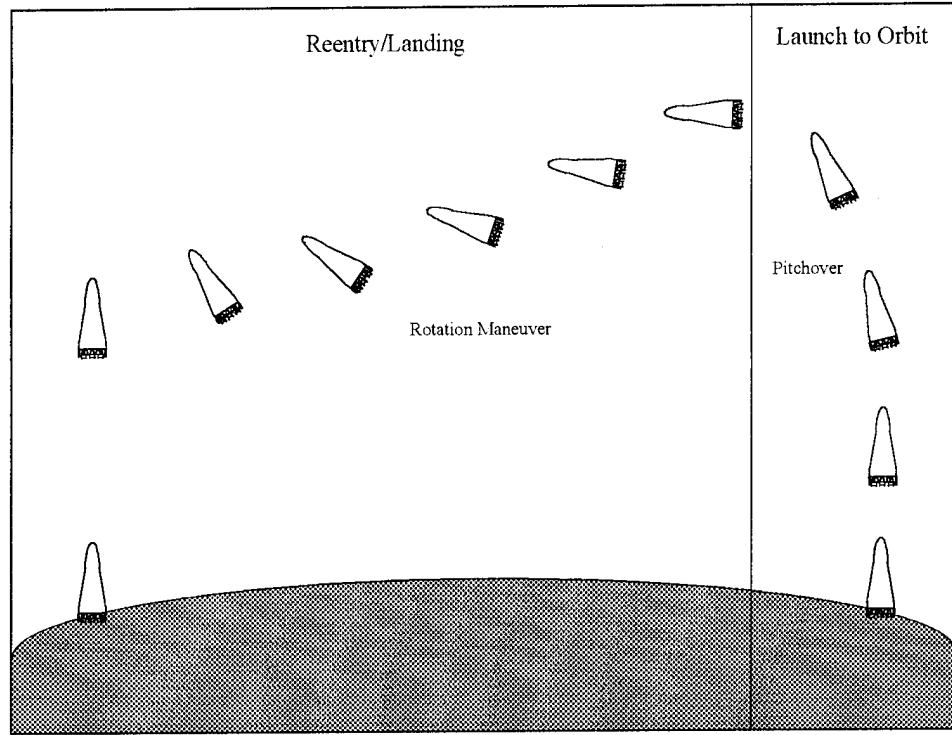
Rotation Maneuver

Figure 1-2 Typical Launch and Landing Rotation Maneuver

1.3 Control Background Since the late 1880's when Floquet developed the first solutions for time periodic linear systems, there has been extensive work done in the field, especially in the area of celestial mechanics with the restricted three body problem. Most of this work has concentrated on determining the stability of a given orbit rather than controlling said orbit.

Literature on control theory, while plentiful, tends to focus on the linear constant-coefficient case. Although many systems can be linearized, few systems can be specified

independent of time, which restricts the use of control. Breakwell et al. [2] dealt with the control of unstable periodic orbits through use of the Linear Quadratic Regulator. In their work, Wiesel and Calico [12] designed a method for single pole placement in periodic systems. Some years later, Wiesel [14] developed a method for dictating the value for a single pole in a general time-dependent linear system. Recently, Wiesel has extended the pole placement algorithm to allow full Lyapunov exponent determination in a general time-dependent linear system. This method also allows specification of the principal dynamical directions, and will be the main focus of this study.

1.4 Principal Accomplishments The principal accomplishments of this research are:

- Development of a 6 state trajectory design algorithm for a Delta Clipper-like reentry vehicle.

- Successful application of Wiesel's full pole placement algorithm for several example reentry trajectories.

- Discovery of algorithm difficulties in controlling extended trajectory arcs.

- Detection of problems in algorithm calculation of a finite gain matrix.

5

II. TRAJECTORY MODEL DESIGN

2.1 Assumptions   In order to model the reentry trajectory accurately, several general assumptions must apply. They are as follows.

1. The vehicle specifications will be those listed in Section 1.2.

2. The control variables will be roll and angle of attack.

3. The aerodynamic model, from which the coefficients of drag and lift, C_D and C_L are determined, is accurate.

4. The atmospheric model described in Section 2.4 adequately describes the atmosphere through which the reentry vehicle will travel.

5. The 6 dimensional state vector, described in the next section, is sufficient to model the dynamics of the reentry trajectory.

2.2 Equations of Motion   The dynamics model we use for the reentry of a vehicle into the atmosphere is based on a six dimensional state space. Vinh's [11:19-27] formulation of the equations of motion is used in the following development. We start with the three parameters which define the motion of the vehicle with respect to the center of the earth: position vector, $\vec{r}$, velocity vector, $\vec{v}$, and mass, m. Since the reentry vehicle travels in the earth centered inertial frame, the position vector of the vehicle, $\vec{r}$, is defined by its magnitude, r, the longitude, θ, and the latitude, ϕ,. We also define γ as the flight path angle or the angle between the local horizontal plane and the velocity vector, $\vec{v}$, and ψ as the heading or the angle between the local parallel of latitude and the projection of the velocity vector, $\vec{v}$, on the horizontal plane. We now have the six components of the state space as follows.

r - magnitude of the radius vector
θ - longitude
φ - latitude
v - speed
γ - flight path angle
ψ - heading

At this point, we must determine the equations of motion for the state space vector. At a given point in time the vehicle is subject to the following force:

$$\vec{F} = \vec{T} + \vec{A} + m\vec{g}.$$

$\vec{T}$ is defined as the force due to thrust, while $\vec{A}$ is the aerodynamic force, the quantity $m\vec{g}$ is the force due to gravity. Since we are assuming an unpowered reentry, $\vec{T} = \vec{0}$ resulting in the equation,

$$\vec{F} = \vec{A} + m\vec{g}.$$

Since the vehicle will be moving about within the inertial earth centered frame, we want to define a rotating frame such that the x axis is aligned with the position vector, the y axis is in the equatorial frame with positive values toward the direction of motion, and the z axis completes the right handed system, as seen in Figure 2-1. We can therefore write the position and velocity vectors as follows:

$$\vec{r} = r\vec{i} \qquad\qquad (2\text{-}0)$$

$$\vec{v} = (v Sin\gamma)\vec{i} + (v Cos\gamma Cos\psi)\vec{j} + (v Cos\gamma Sin\psi)\vec{k}. \qquad (2\text{-}1)$$
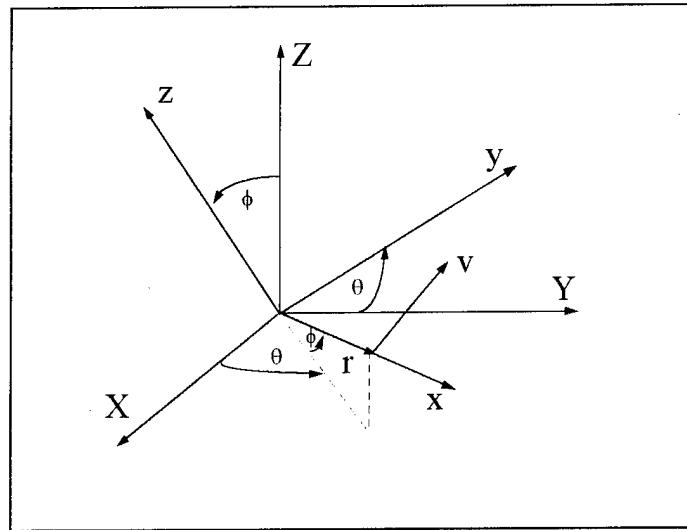
Figure 2-1. - Reference Frames

We know that in the rotating system the following definition of velocity is valid,

$$\vec{v} = \frac{d\vec{r}}{dt} = \vec{\omega} \times \vec{r},$$

with the value of $\vec{w}$ being defined as :

$$\vec{\omega} = (Sin\phi \frac{d\theta}{dt})\vec{i} - (\frac{d\theta}{dt})\vec{j} + (Cos\phi \frac{d\theta}{dt})\vec{k}.$$

Since we know that

$$\frac{d\vec{r}}{dt} = (\frac{dr}{dt})\vec{i} + (\frac{d\vec{i}}{dt})r, \qquad (2\text{-}2)$$

where

$$\frac{d\vec{i}}{dt} = \vec{\omega} \times \vec{i} = (Cos\phi \frac{d\theta}{dt})\vec{j} + (\frac{d\phi}{dt})\vec{k},$$

we can equate equations 2-1 and 2-2 to get the following three equations of motion:

8

$$\frac{dr}{dt} = v\,Sin\gamma$$

$$\frac{d\theta}{dt} = \frac{v\,Cos\gamma\,Cos\psi}{r\,Cos\phi}$$

$$\frac{d\phi}{dt} = \frac{v\,Cos\gamma\,Sin\psi}{r} \,.$$

Now if we take the derivative of equation 2-0 and perform a similar procedure, we can come up with the following equations of motion for the last three states:

$$\frac{dv}{dt} = -\frac{D}{m} - g\,Sin\gamma$$

$$\frac{d\gamma}{dt} = \frac{L\,Cos\sigma}{vm} - \frac{g\,Cos\gamma}{v} + \frac{v}{r}Cos\gamma$$

$$\frac{d\psi}{dt} = \frac{L\,Sin\sigma}{vm\,Cos\gamma} - \frac{v}{r}Cos\gamma\,Cos\psi\,Tan\phi \,,$$

with D, L, and σ being the values of drag, lift and roll respectively. Roll and angle of attack, α, are the two control variables which we will be able to manipulate in this problem. Angle of attack is defined as the angle between the v_1 component of the velocity vector and the b_1 axis of the vehicle as defined in Appendix A. Roll is defined as the angle between the local vertical plane (containing the radius vector, $\vec{r}$, and the velocity vector, $\vec{V}$) and the aerodynamic plane (containing the aerodynamic force, $\vec{A}$, and $\vec{V}$). Drag and lift will be functions of velocity and cross sectional area of the vehicle, angle of attack and

density of the atmosphere as follows:

$$D = \frac{\rho S C_D(\alpha) V^2}{2}$$

$$L = \frac{\rho S C_L(\alpha) V^2}{2}.$$

The angle of attack can be used to determine the coefficients of drag and lift, C_d and C_L. The method of calculating the coefficients of lift and drag is contained in the next section.

2.3 Coefficients of Lift and Drag   In order to determine the coefficients of lift and drag, we must first determine the shape of the reentry vehicle. Using the vehicle shown in Figure 1-1, we can extrapolate a model for the vehicle which is represented by a cone with an 8° cone half angle, χ, and a base diameter of 12.19 meters (see Figure A-1). Appendix A contains the derivation of the following equations which allow us to determine C_D and C_L based upon the angle of attack of the vehicle.

$$C_D A = L^2 \int_{\zeta_-}^{\zeta_+} \left\{ \begin{array}{l} 2[\text{Sin}(\chi)\text{Cos}(\alpha) + \text{Cos}(\zeta)\text{Cos}(\chi)\text{Sin}(\alpha)]^2 \dfrac{\text{Tan}(\chi)}{\text{Cos}(\chi)} \\[2mm] x \quad [\text{Sin}(\chi)\text{Cos}(\alpha) + \text{Cos}(\chi)\text{Cos}(\zeta)\text{Sin}(\alpha)] \end{array} \right\} d\zeta$$

$$C_L A = L^2 \int_{\zeta_-}^{\zeta_+} \left\{ \begin{array}{l} 2[\text{Sin}(\chi)\text{Cos}(\alpha) + \text{Cos}(\zeta)\text{Cos}(\chi)\text{Sin}(\alpha)]^2 \dfrac{\text{Tan}(\chi)}{\text{Cos}(\chi)} \\[2mm] x \quad [\text{Sin}(\chi)\text{Sin}(\alpha) - \text{Cos}(\chi)\text{Cos}(\zeta)\text{Cos}(\alpha)] \end{array} \right\} d\zeta$$

$$\text{where} \quad \zeta = \left\{ \begin{array}{ll} \pi & \text{when} \quad \alpha < \chi \\ \text{Cos}^{-1}[-\text{Tan}(\chi)\text{Ctn}(\alpha)] & \text{when} \quad \alpha \geq \chi \end{array} \right\}$$

These equations allow us to calculate a C_D and a C_L for any angle of attack if we are given a cone half angle, ζ. For the 8 degree cone half angle of our vehicle, this converts to the graph of C_D and C_L versus angle of attack in Figure 2-2.
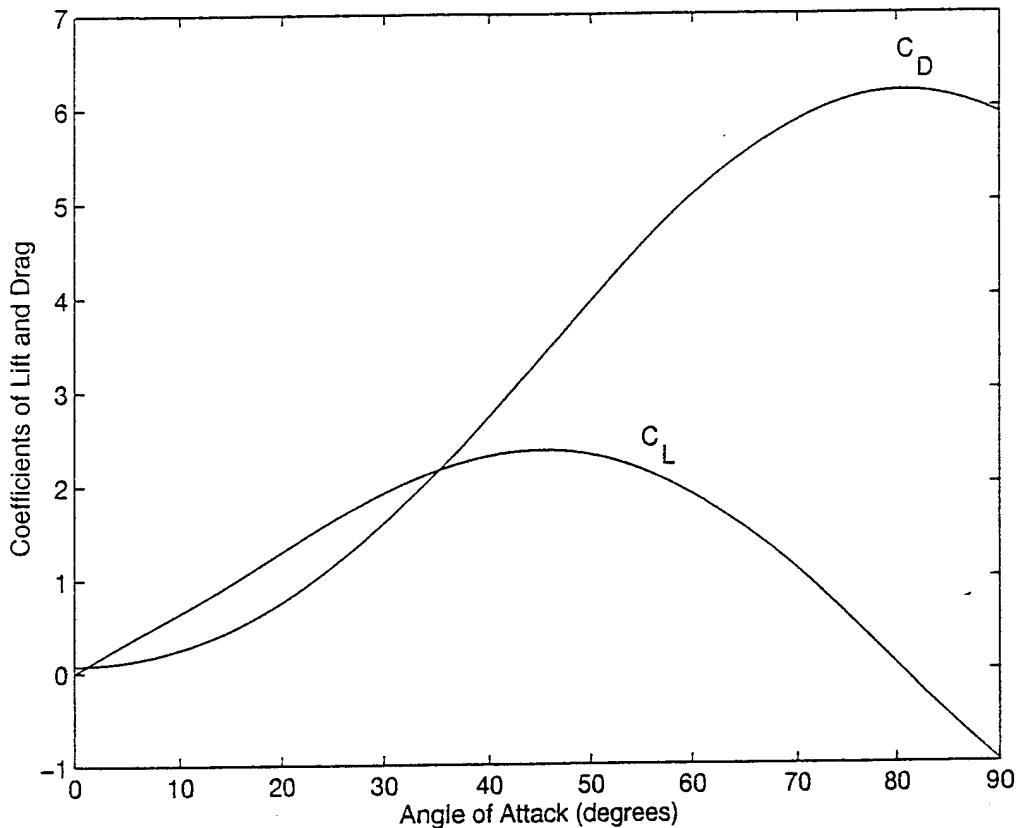
Figure 2-2 C_L and C_D vs Angle of Attack

2.4 Atmospheric model   Once the coefficients of lift and drag have been determined, it is necessary to find the density of the atmosphere at the altitude of the reentry vehicle. We use the method developed by Regan [10:21-45] which utilizes a linear model of the atmosphere, divided into 21 discrete sections from 0 to 700 km. The model assumes

several characteristics of the atmosphere including thermodynamic fluid behavior and equilibrium under both pressure and gravitational forces. These two characteristics result in the following equations:

$$\frac{dP}{dZ} = -\rho g$$

$$PV = R * T.$$

where
g = acceleration due to gravity
P = pressure
R = gas constant for air
ρ = density of air
T = temperature
V = volume

These equations lead to an atmosphere with several break points indicating changes in the slope of density curves. Table 2-1 gives the base parameters and the lapse rate which defines the changes in the respective regions. To determine the actual density at an altitude we use the following equations:

If Lapse Rate = 0

$$\rho = \rho_i \exp\left\{-\left[\frac{g_0(Z - Z_i)}{RT_{M_i}}\right]\left[1 - \frac{b}{2}(Z - Z_i)\right]\right\}$$

If Lapse Rate $\neq$ 0

$$\rho = \rho_i\left[\left(\frac{L_{Z_i}}{T_{M_i}}\right)(Z - Z_i) + 1\right]^{-\left\{\left(\frac{g_0}{RL_{Z_i}}\right)\left[\frac{RL_{Z_i}}{g_0} + 1 + b\left(\frac{T_{M_i}}{L_{Z_i}} - Z_i\right)\right]\right\}} \exp\left\{\left(\frac{g_0 b}{RL_{Z_i}}\right)(Z - Zi)\right\}$$

where i indicates the value at the bottom of the respective region listed in Table 2-1.

12

This model represents a standard atmosphere. It does not take into account any daily variations or changes due to unpredicted solar activity. It also ignores the effects of atmospheric winds on the pressure in a given area.

Layer Index	Geometric Altitude (km)	Molecular Temperature (K)	Lapse Rate K/km
0	0.0	288.15	-6.5
1	11.0102	216.65	0.0
2	20.0631	216.65	+1.0
3	32.1619	228.65	+2.8
4	47.3501	270.65	0.0
5	51.4125	270.65	-2.8
6	71.8020	214.65	-2.0
7	86.0	186.10	+1.7
8	100.0	210.65	+5.0
9	110.0	260.65	+10.0
10	120.0	360.65	+20.0
11	150.0	960.65	+15.0
12	160.0	1110.65	+10.0
13	170.0	1210.65	+7.0
14	190.0	1350.65	+5.0
15	230.0	1550.65	+4.0
16	300.0	1830.65	+3.3
17	400.0	2160.65	+2.6
18	500.0	2420.65	+1.7
19	600.0	2590.65	+1.1
20	700.0	2700.65	

TABLE 2-1   21 Layer Atmosphere

2.5 State Space Version of the Equations of Motion   The equations of motion for a nonlinear time-dependent system are usually written in the following form:

$$\dot{X} = f(X,U,t).$$

X is the vector of state variables, U is the vector of control variables, and t is time. Since we require a linear system for this particular control algorithm, this system can be rewritten as a displacement off a given trajectory $X_0(t)$ and nominal control $U_0(t)$.

$$\left[\dot{X}(t) - \dot{X}_0(t)\right] = \left(\frac{\partial F}{\partial X}\right)_{X_0 U_0} \left[X(t) - X_0(t)\right] + \left(\frac{\partial F}{\partial U}\right)_{X_0 U_0} \left[U(t) - U_0(t)\right]$$

For ease of notation, we define the following values.

$$A(t) = \left(\frac{\partial F}{\partial X}\right)_{X_0 U_0} \qquad\qquad B(t) = \left(\frac{\partial F}{\partial U}\right)_{X_0 U_0}$$

$$x = X(t) - X_0(t) \qquad\qquad u = U(t) - U_0(t)$$

The component equations for the A and B matrices are listed in Appendices C and D respectively. The last two equations define x as the first order deviation from the nominal trajectory, and u as the first order deviation from the control theory. In order to "control" this system, we wish to choose u(t) such that X(t) is linearly stable.

In order to efficiently evaluate all possible trajectories, we define a matrix, Φ, called the state transition matrix which allows us to view trajectories near a nominal trajectory. Further explanation of Φ and its use is described in Appendix B.

In order to update the initial Φ matrix, we must determine an equation of motion for $\dot{\Phi}$, typically called the equation of variation. Experience and the definition of the Φ matrix tell us that this equation is $\dot{\Phi} = A\Phi$. A more extensive development of this equation can be seen in Appendix B. The A matrix is the same one defined above.

14

2.6 Trajectory Specifications   With the equations of motion determined, we are able to propagate the vehicle through its trajectory from any initial condition. In order to accomplish the entire integration, we must first design a trajectory. Basically, this involves setting the initial conditions and the control law based on the probable reentry point and the characteristics of the vehicle. Since in this example we are using a DCX-like launch vehicle, we assume that we will be able to control both angle of attack and roll using the control system of the reentry vehicle. This allows us to specify these two control variables at any given time. The control law we will be using is very simple; the law checks to see if the vehicle is at a pull-up point. This is the point in the trajectory where the aerodynamic forces cause enough lift on the vehicle to cause it to increase in altitude. If it is, from that point on the angle of attack is adjusted so that it produces just enough lift to keep the vehicle in level flight. The roll is maintained at its initial value. We look at five trajectories in order to fully validate the flexibility of the control algorithm. The first trajectory is a ballistic trajectory with the vehicle reentering with both control variables, roll and angle of attack, set equal to zero.

The second trajectory has roll set equal to zero for the entire flight, while the pitch is maintained at the initial value until the vehicle reaches the point at which it begins to pull up. At this point the angle of attack is adjusted so that the vehicle maintains a level flight for as long as possible. The initial angle of attack will be selected to maximize the flight time. This trajectory is designed to give us the longest possible time at a higher altitude, thereby avoiding the aerodynamic forces the vehicle is subject to at lower altitudes. Since the only way the vehicle can maintain level altitude is by generating lift, it experiences

some aerodynamic forces. However, staying higher until its velocity has decreased reduces the overall negative effects of reentry such as heating and deceleration.

The third trajectory is identical to the second trajectory, except the roll is set a specific non-zero value for the entire reentry. This maintains the benefit of less aerodynamic forces while allowing the vehicle to adjust for any cross range error which might be present. The fourth trajectory has zero initial angle of attack and 0.5 radian initial roll. This allows us to determine how the algorithm handles roll with no angle of attack. The final trajectory has no initial roll and a 1.5 radian initial angle of attack. This allows us to evaluate how the algorithm will handle large angles of attack.

With the trajectory designed, we will iterate the state vector and the Φ matrix through the entire flight. The trajectory is terminated when the radius drops below the radius of the earth. Upon termination of the trajectory, the final Φ matrix is used to determine the stability of the trajectory (see next section). All these trajectories are simplistic, in that they do not contain any post-reentry maneuvering independent of the control law we have established for angle of attack. This simplicity is due to the fact that the trajectories are being used only to observe the control algorithm discussed in the next section and therefore represent certain extremes of the possible trajectories.

III. Control Algorithm

3.1 Introduction   Control theory often deals with the control of constant coefficient

linear systems. Some extensive work has also been done with time periodic systems.

However, Wiesel [14] has recently developed a modal decomposition for the general time-

dependent system and formulated a method for moving a single pole to any desired

location. A later Wiesel paper [13] details a method for placing all the control system's

Lyapunov exponents and dynamical directions. The general features of this control

method are detailed below.

3.2 Lyapunov Exponents   The stability of a general system is determined by its

Lyapunov exponents which are defined as follows:

$$L_i = \frac{1}{t_f - t_0} \log \frac{\left| \Phi(t_f, t_0) e_i(t_0) \right|}{\left| e_i(t_0) \right|}, \qquad (3\text{-}0)$$

and are maximized over all initial displacements, $e_i(t_0)$. The $e_i(t_0)$ vectors represent the

maximums in the growth rate of the norm of the final displacement vector $\left| x(t_f) \right|$ with

respect to the initial displacement vector $x(t_0)$. We would usually include a limit as t_f goes

to infinity in this definition of a Lyapunov exponent, but since we are dealing with a

control algorithm, we need to restrict ourselves to finite times. In order to be able to

control a system, we must be able to predict its future behavior in order to be able to

affect its eventual outcome. In a chaotic trajectory we are only able to predict the future

for finite periods of time.

17

We must constrain maximization described earlier in order to avoid a large initial displacement resulting in a final displacement too large to handle. To accomplish this, we simply assume the magnitude of the principal dynamical direction vectors, **u** and **v**, to be unity, such that:

$$|e_i(t_0)| = |v| = 1 = |e_i(t_f)| = |u|.$$

3.3 Algorithm Development   In their work, Bryson and Ho [3] develop the concept of a Linear Quadratic Regulator (LQR) used below. We start with the following formulation of the system developed from the above equations:

$$\dot{x} = A(t)x + B(t)u. \qquad (3\text{-}1)$$

We then create a performance index which we will attempt to minimize. In normal LQR's, the matrices S_f, C, and D are positive definite and discourage deviations from the nominal trajectory final conditions, deviations from the nominal trajectory and the use of control, respectively. We are modifying the LQR so that we are actually specifying the Lyapunov exponents of the system, therefore we are no longer able to ensure that these matrices, especially S_f, will be positive definite.

$$J = \frac{1}{2}x_f{}^T S_f x_f + \frac{1}{2}\int_{t_0}^{t_f}\left(x^T C x + u^T D u\right)dt \qquad (3\text{-}2)$$

By manipulating equation 3-1, we are able to incorporate Lagrange multipliers creating the following equation:

$$J' = \frac{1}{2}x_f{}^T S_f x_f + \frac{1}{2}\int_{t_0}^{t_f}\left(x^T C x + u^T D u + 2\lambda^T\left[Ax + Bu - \dot{x}\right]\right)dt.$$

If we integrate the $\dot{x}$ by parts we get

$$J' = \frac{1}{2}x_f^{\,T}S_f x_f - \lambda^T x\big|_{t_0}^{t_f} + \frac{1}{2}\int_{t_0}^{t_f}\left(x^T C x + u^T D u + 2\lambda^T\left[Ax + Bu\right] + 2\dot{\lambda}^T x\right)dt .$$

Since we are trying to minimize J', we must zero the first variation of J', $\delta J' = 0$, which, along with equation 3-1, results in the following equations:

$$\dot{x} = A(t)x + B(t)u \qquad\qquad\qquad \textbf{(3-3)}$$

$$\dot{\lambda} = -A^T\lambda - C^T x \qquad\qquad\qquad \textbf{(3-4)}$$

$$u = -D^{-1}B^T\lambda \qquad\qquad\qquad \textbf{(3-5)}$$

$$\lambda_f = S_f^{\,T} x_f . \qquad\qquad\qquad \textbf{(3-6)}$$

For this particular problem, we ignore the C matrix. Rather than simply discouraging the deviation from the nominal trajectory, we will actually specify the stable Lyapunov exponents for the closed loop system. This alters equation 3-4 into the equation

$$\dot{\lambda} = -A^T\lambda . \qquad\qquad\qquad \textbf{(3-7)}$$

Combining equations 3-3 and 3-5 leads to another formulation of the derivative of the state vector:

$$\dot{x} = Ax - BD^{-1}B^T\lambda . \qquad\qquad\qquad \textbf{(3-8)}$$

We now want to solve the above equations as a boundary value problem. In most cases, we have initial conditions $x(t_0)$ and the freedom to choose one more set of boundary values. The logical choice is equation 3-6, which is then used in its general form, $\lambda = Sx$, along with equation 3-7 to yield

$$\dot{S}x + S\dot{x} = -A^T Sx ,$$

which when combined with equation 3-8 results in the next equation,

19

$$\dot{S} = SBD^{-1}B^TS - A^TS - SA.$$

This equation is called the matrix Ricatti Differential equation and can be propagated independently of the closed loop linear system and the Lagrange multiplier equations. Since we know the final value, S_f, we are able to use the Ricatti equation to sweep back through the trajectory and determine S_0. This in turn yields $\lambda(t_0)$ from equation 3-6 and the initial conditions. Now equations 3-7 and, subsequently, 3-3 can be integrated forward through the designated period of time. This algorithm is called the dual sweep method. It also allows us to rewrite equation 3-4 in the following form:

$$\dot{x} = \left(A - BD^{-1}B^TS\right)x.$$

Using equation 3-5, we define the following value as the gain matrix,

$G(t) = -D^{-1}B^TS$, which allows us to write equation 3-3 in this form:

$$\dot{x} = \left(A + BG\right)x.$$

If we are able to determine the values of the G matrix with respect to time, these values can be input into the reentry vehicle's control system allowing the vehicle to actually fly the specified reentry trajectory.

Previously, we assumed that the final value of S was known. Instead of simply defining how much we want the final conditions to deviate from the nominal final conditions, we would rather establish stability conditions on the dynamics of the system. One measure of the stability of a given path of the trajectory is its Lyapunov exponents. It is a fairly simple exercise to determine the open loop Lyapunov exponents. Since we know the open loop system follows the restriction,

$$\dot{\Phi}_x = A\Phi_x,$$

where $\Phi_x(t_0) = I$, and I is the identity matrix. By decomposing the Φ_x matrix at $t=t_f$, we are left with singular vectors **u** and **v** and diagonal matrix W of the form

$$\Phi_x(t_f) = uWv^T.$$

The vector **v** is an orthonormal vector that gives the directions that the initial conditions of the given trajectory differ from the initial conditions of the reference trajectory in state space on a unit sphere at time $t=t_0$. This matrix propagates through the trajectory in the directions on the ellipsoid defined by the orthonormal **u** matrix at time $t=t_f$. The values of the components in the diagonal W matrix are the axis lengths of the ellipsoid at $t=t_f$. The Lyapunov exponents are then defined as a variation of equation 3-0 or

$$L_i = \frac{1}{t_f - t_0} \log(w_i).$$

The above equations are valid for both the open and closed loop cases. Since we want to be able to specify what the closed loop Lyapunov exponents will be, we will simply set the closed loop principal dynamical directions equal to the open loop values such that, $u_O = u_C$ and $v_O = v_C$. We know the open loop Lyapunov exponents, $L_{i,o}$, and we will specify the closed loop Lypunov exponents, $L_{i,c}$. Using equations 3-7 and 3-8 and taking the partial derivatives with respect to initial conditions, $x(t_0)$, we get the following result:

$$\frac{d}{dt}\Phi_{x,C} = A\Phi_{x,C} - BC^{-1}B^T\Phi_\lambda \qquad \text{(3-9)}$$

$$\frac{d}{dt}\Phi_\lambda = -A^T\Phi_\lambda, \qquad\qquad (3\text{-}10)$$

where $\Phi_{x,c} = \partial x(t)/\partial x(t_0)$

and $\Phi_\lambda = \partial \lambda(t)/\partial x(t_0)$

These equations then form a linear boundary value problem. To solve the problem for the values of $\Phi_\lambda(t_0)$, we must integrate equations once to get the open loop solution and then (order)^2 or 36 times to get the numerical partial derivatives, $\partial\Phi_{x,c}(t_f)/\partial\Phi_\lambda(t_0)$. Once we have these values, one iteration of the Newton Rhapson method,

$$\Phi_\lambda(t_0) = \left[\frac{\partial\Phi_{x,c}(t_f)}{\partial\Phi_\lambda(t_0)}\right]^{-1}\left(\Phi_{x,c}(t_f) - \Phi_{x,o}(t_f)\right),$$

will yield the value for $\Phi_\lambda(t_0)$ for the given value of $\Phi_{x,c}(t_f)$.

Previously we implied that by specifying the closed loop Lyapunov exponents, we were in effect eliminating the need to define an S_f matrix. Now we can prove this assumption is valid. Since we are able to calculate the value of $\Phi_\lambda(t_0)$, using equation 3-6 and the initial conditions give us the values of S_0, we can then integrate forward using the Ricatti equation to get S_f. So, S_f is implicitly determined by our choice of the Lyapunov exponents and the principal dynamical directions. Recall that since we are using a modified LQR, there is not guarantee that S_f will be positive definite as it would be in a normal LQR.

IV. Implementation of the Control Algorithm

4.1 Introduction   There are basically three programs which are required to implement Wiesel's control algorithm. The trajectory design program, DESIGN, the open loop calculation program, FIRST, and the boundary value program, BVP. In order to avoid problems which arose in trying to decompose matrices and solve linear equations that were written in terms of metric units, most units in the code are handled in non-dimensional units. These units which we will call Distance Units (DUs) and Time Units (TUs) are defined below.

$$1DU = 6378.145 km$$
$$1TU = 806.8118744 sec$$
$$1\frac{DU}{TU} = 7.90536828\frac{km}{sec}$$

The only subroutine which uses metric units is the atmospheric model which is part of the dynamics model and will be described below. The flow chart for the three different programs can be found in Appendices E, F, and G. The main characteristics of the programs and subroutines listed below can be found in Appendix H and the input files required by each program can be found in Appendix I.

4.2 Trajectory Design Program   In order to test the control algorithm, we must first set up the computer model of the trajectory dynamics. The trajectory design program, DESIGN, accepts the initial conditions of the state vector, control variables, and other miscellaneous parameters from an input file. It then calls a routine developed by Dr Wiesel, called AERO, which accepts the angle of attack of the vehicle, uses a reference

table derived by the method detailed in Appendix A, and outputs the coefficients of drag and lift, C_D and C_L, and derivatives of these values with respect to angle of attack. At this point, DESIGN provides the maximum lift angle of attack, causing AERO to output the maximum lift C_L and C_D.

The code then initializes an integration routine called HAMING. This subroutine is an ordinary differential equations integrator using a fourth-order predictor-corrector algorithm. The code saves the last four values of the state vector and Φ matrix and uses these to determine the predicted value of the state vector and the Φ matrix. This predicted value is then corrected using the equations of motion and the A matrix to find the new value of the state vector and Φ matrix. Since we only provide the trajectory design program with one set of initial conditions rather than the four required by the Haming subroutine, an algorithm called a Picard iteration is used to find the other three. This process is not used for the entire iteration since it is much slower than the Haming algorithm. Within the HAMING routine, a subroutine called PHIRHS is implemented. PHIRHS calls a dynamics routine and uses the output of this to calculate the equations of motion for the state vector and Φ matrix which HAMING in turn uses to propagate the orbit.

The dynamics subroutine that PHIRHS calls is named DYNAM. After defining some initial parameters, this subroutine calls the AERO subroutine described earlier and determines the C_L and C_D for the current angle of attack. The routine then checks to see if the vehicle is in a pull up maneuver. If it is, DYNAM determines the new C_L and C_D, if it is not, the program checks to see if the vehicle is within an altitude range for which the

atmospheric model is valid. If the vehicle is outside the acceptable altitude range (0-700km), the code outputs that the model is not valid. If the vehicle is within the acceptable range, DYNAM calls the atmospheric model subroutine called ATM. This routine first converts the altitude and density at sea level to metric units. It then determines which of the 21 layers of the atmosphere the vehicle is in and calculates the density, pressure and temperature at the current altitude. These values are converted back to non-dimensional units and returned to DYNAM. The code determines the current values for the equations of motion for the state vector and the values of the A and B matrices.

Once HAMING has been initialized, it is run a pre-selected number of times. After each run of HAMING, the program checks to see if the vehicle has reached the point where it is starting to pull up (i.e. an increase in altitude). If it has, the C_L is adjusted so that the vehicle remains in level flight; HAMING is reinitialized; and a flag is initiated to ensure that C_L will be continuously adjusted for level flight. If a pull up has not occurred yet, the iteration continues.

At this juncture the program checks for whether the vehicle has dropped below a minimum height signifying impact. The impact value can be set at any value (ie sea level or some point above to represent the point at which a Delta Clipper-like vehicle would perform its rotation to vertical maneuver prior to landing). After this check, the necessary variables are written to several output files. The trajectory design program creates numerous files which can be used to graph different combinations of the state variables. It also creates an output file called FIRST.IN which is used in the next program, FIRST.

This file contains the number of iterations of HAMING that have been accomplished as well as the initial conditions and parameters that were input to DESIGN. Three other files that will be used in both FIRST and BVP are created as well. These files, CONTROL, CONTROL2.OUT, and CONTROL3.OUT, contain a control history of the trajectory, including the time, pitch, roll, C_D, and C_L values at each iteration of HAMING.

4.3 Open Loop Value Program   Once the trajectory has been designed, we are able to implement the control algorithm. The first program that accomplishes this is appropriately called FIRST. This program accepts the output of DESIGN, and iterates through the trajectory, updating the state vector and the Φ matrix. It then uses the program SVDCMP, which performs a singular value decomposition of the Φ matrix, to get the orthonormal dynamical direction vectors, **u** and **v** and the W matrix. From the W matrix, it calculates the open loop Lyapunov exponents. Since the next program implements the boundary value portion of the control algorithm, FIRST outputs all the initial conditions and parameters to a file called BVP.IN along with two copies of the open loop Lyapunov exponents , the open loop **u** and the open loop **v** vectors. Two copies are written to this file because the input file for the boundary value program, BVP, requires both the open loop values and the required closed loop values. Since the closed loop **u** and **v** vectors will be set equal to their open loop values for our purposes, it is convenient to simply edit the BVP.IN file prior to running BVP so that the second Lyapunov exponents are our desired closed loop values.

4.3 Boundary Value Problem Program The program BVP needs both the open loop Lyapunov exponents and principal directions, as well as the desired closed loop Lyapunov exponents and principal directions in order to set up the boundary value problem so, as stated above, we now edit BVP.IN to include the desired closed loop values of the Lyapunov exponents. Once this is done, BVP accepts the input file BVP.IN and constructs a desired closed loop Φ matrix based on the closed loop **u** and **v** vectors and the Lyapunov exponents. The program initializes both the Φ matrix and another matrix, called the Φ Lagrangian matrix which is made up of the Lagrangian multipliers. It iterates through the trajectory calculating the open loop Φ and Φ Lagrangian values. The program then iterates through the trajectory (order)^2 or 36 times to construct the Φ Lyapunov numerical partials. This is accomplished by adding a delta value to the initial Φ Lagrangian element and determining the final Φ element after the trajectory is integrated. The value of the final element without perturbation is subtracted from the value with perturbation and the difference is divided by the delta value in the following manner.

$$\frac{\partial \Phi}{\partial \Phi_\lambda} = \frac{\Phi_{Perturbed} - \Phi_{Unpereturbed}}{delta}$$

From these partials, the program calculates the final Φ Lagrangian matrix. This is done by solving the following matrix equation of the partials (Basis), the Φ Lagrangian matrix and the error matrix.

$$(Basis)(\Phi_\lambda) = E$$

$$\text{where} \quad E = \Phi_{Desired} - \Phi_{Unperturbed}$$

27

This results in a Φ_λ at $t=t_0$. The code iterates through the trajectory one final time to validate the solution. During this iteration, the gain matrix is written to an output file along with the time and the value of the state variables at that point in time. After this run through the trajectory, the achieved Φ matrix and the closed loop Lyapunov exponents and **u** and **v** vectors are output.

V. RESULTS

5.1 Reentry Trajectory Alternatives For our purposes, all the trajectories will start with the same initial conditions listed below in Table 5-1. The only values that will be changed are the initial control variables, angle of attack and roll. In order to test the control algorithm on the extremes of possible trajectories, we must first determine what those extremes are.

Radius	6528.145 km
Longitude	0.000 rad
Latitude	0.000 rad
Velocity	7.807 km/sec^2
Flight path Angle	-0.085 rad
Heading	0.000 rad
Mass of the Vehicle	45994.740 kg

Table 5-1 Initial Conditions

It would make sense that the ballistic trajectory (Case 1), in which initial roll and angle of attack are zero, would result in a short trajectory with a high deceleration. From Figure 5-1, we can see that the output of the DESIGN program seems to agree with this. Since the initial roll and angle of attack of zero produce no lift, the vehicle never gets the chance to pull up, so according to our original control law, the angle of attack never changes. Therefore, we get a smooth short trajectory as seen in Figure 5-1, an altitude vs range plot, and Figure 5-2, an altitude vs time plot. There is a constant roll of zero so we see no crossrange component in the trajectory.
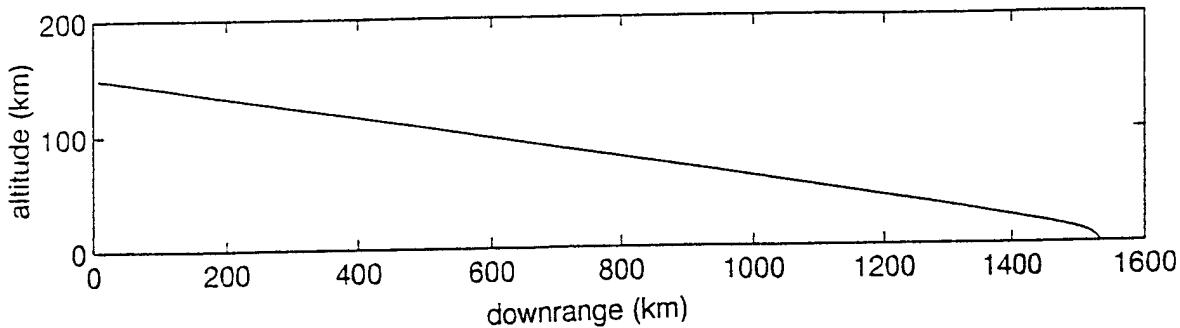
Figure 5-1 Case 1: Altitude vs Range
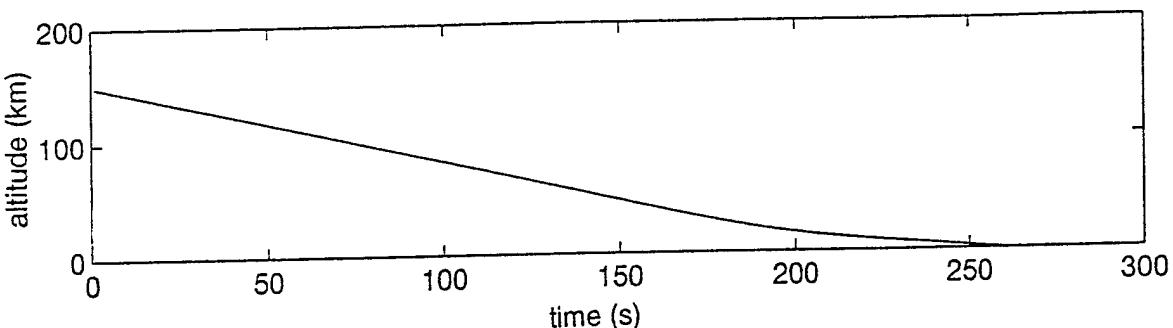
Figure 5-2 Case 1: Altitude vs Time

From the speed vs time graph in Figure 5-3, we can see that there is practically no speed change until about 175 seconds. At this point we get significant reduction in speed and the expected large deceleration, shown in Figure 5.4. This is caused by the dominance of the aerodynamic forces at this altitude, which result in large amounts of drag on the vehicle producing a drop in velocity. To decrease the effect of the atmosphere on the vehicle, we would rather keep the vehicle higher for a longer period of time.

Intuitively, it seems that the best angle of attack to choose, in order to keep the vehicle at high altitudes for as long as possible, would be the angle of attack which causes the maximum lift. The maximum lift angle of attack, chosen from the data file that

30
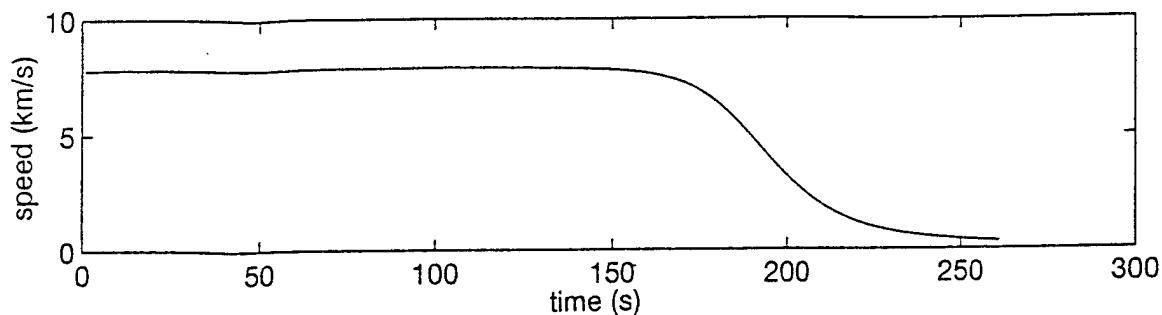
Figure 5-3 Case 1: Speed vs Time
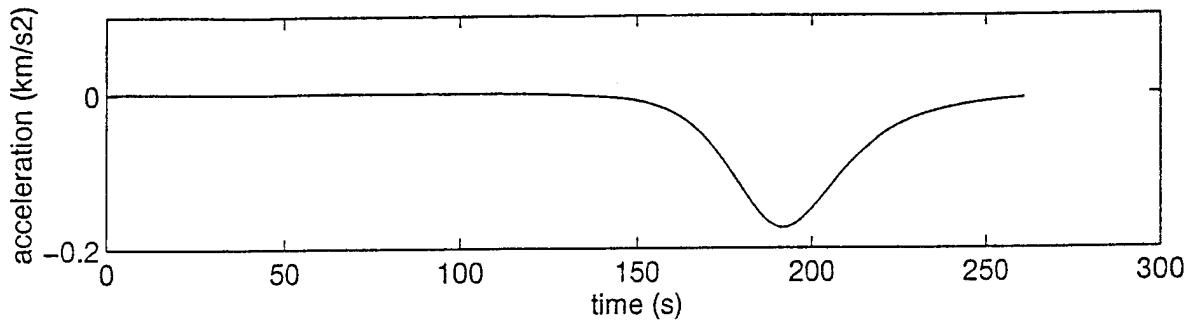
Figure 5-4 Case 1: Acceleration vs Time

produced Figure 2-2, is 0.7893 radians. Figures 5-5 through 5-8 show the results of a

DESIGN run with the initial angle of attack set to this value and the roll set to zero.

Comparing these with Figures 5-1 through 5-4, we see that increasing the initial angle of

attack does in fact decrease the deceleration and therefore the heating and stress on the

vehicle. While the initial deceleration occurs at approximately the same time in both

trajectories, it occurs at a higher altitude and is considerably less when the initial angle of

attack is set at the maximum lift angle of attack.
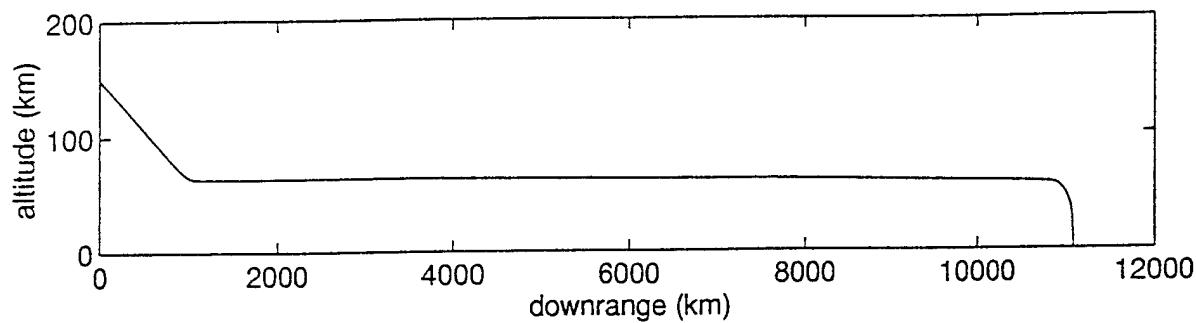
Figure 5-5 Maximum Lift Angle of Attack: Altitude vs Range
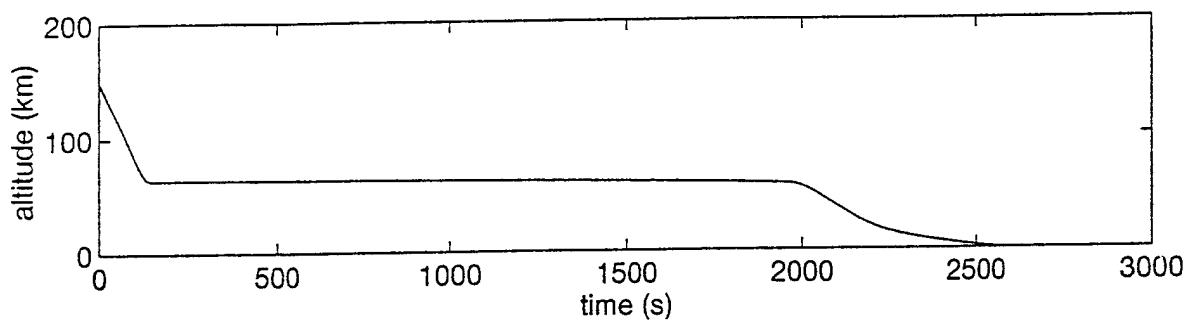
Figure 5-6 Maximum Lift Angle of Attack: Altitude vs Time
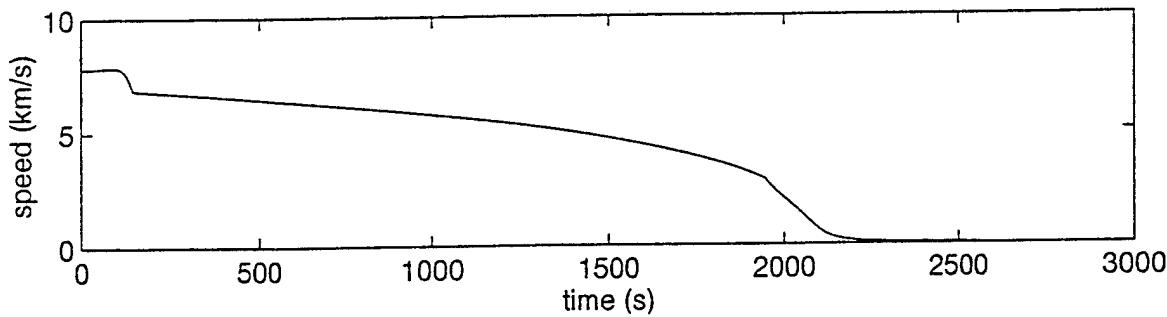
Figure 5-7 Maximum Lift Angle of Attack: Speed vs Time

In order to check the validity of our assumption that the maximum lift angle of

attack will give us the maximum time reentry trajectory, we checked other values near the

maximum lift angle of attack and discovered that the actual maximum time trajectory was
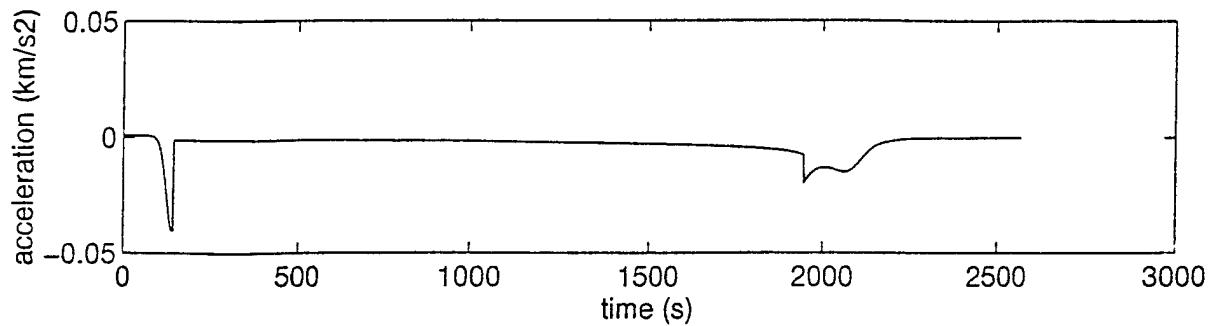
Figure 5-8 Maximum Lift Angle of Attack: Acceleration vs Time

accomplished with an initial angle of attack of 0.325 radians. The results of the DESIGN

run accomplished with this initial angle of attack value can be seen in Figure 5-9 through

5-12 (Case 2). We see that at this angle of attack, we get less deceleration and a longer

trajectory than with the maximum lift angle of attack in terms of both time and range.
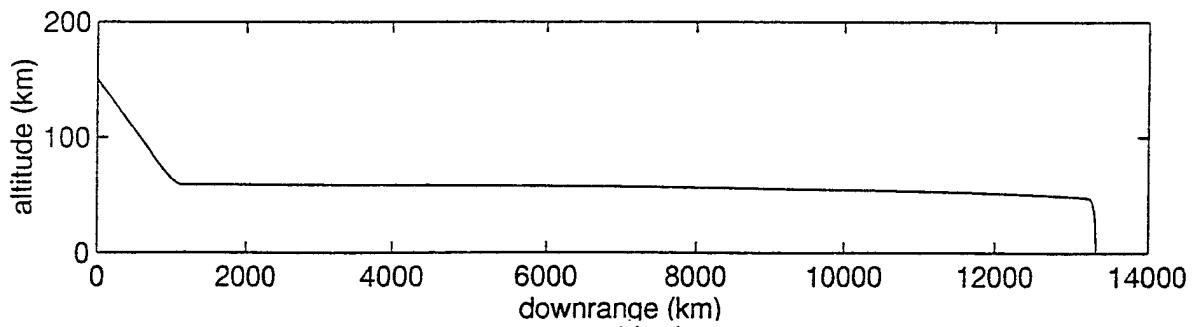
Figure 5-9 Case 2: Altitude vs Range
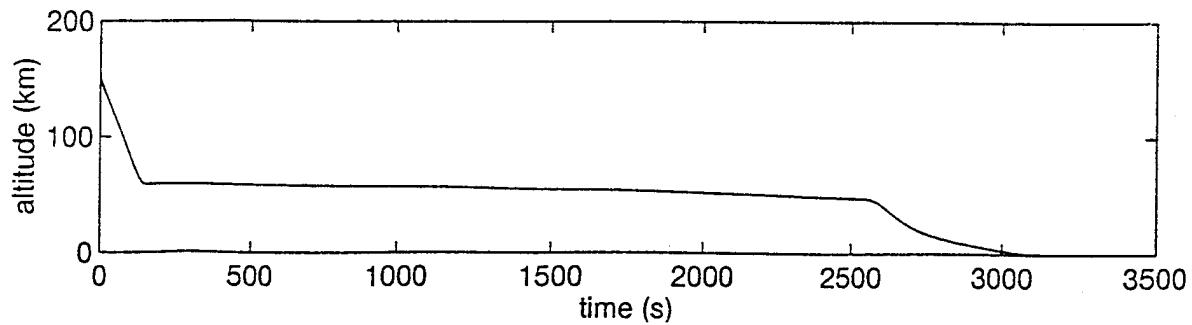
Figure 5-10 Case 2: Altitude vs Time
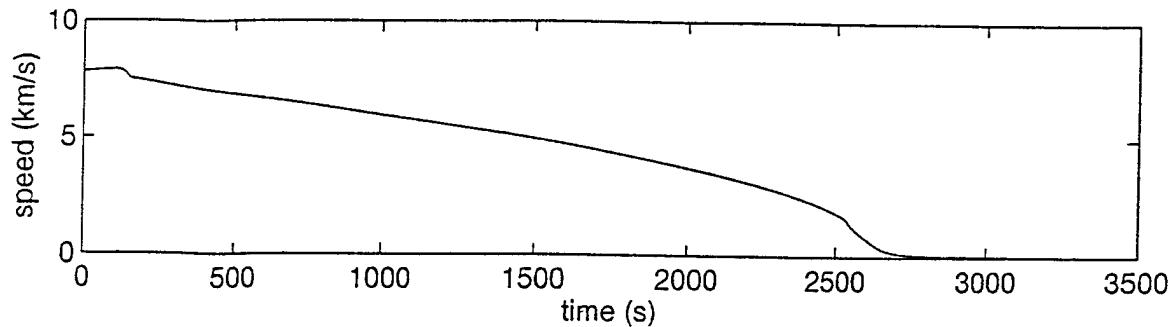
Figure 5-11 Case 2: Speed vs Time
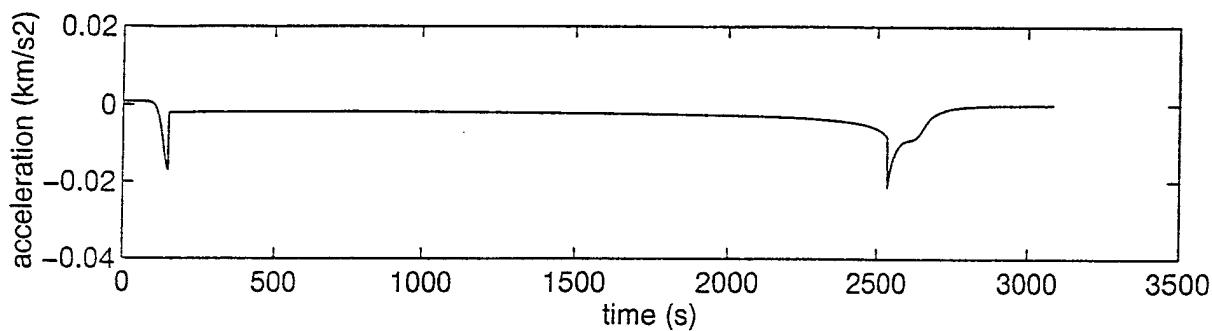
Figure 5-12 Case 2: Acceleration vs Time

To understand why the maximum lift angle of attack does not keep the vehicle at higher altitudes for longer periods of time than a non-maximum lift angle of attack, we must look at the development of the coefficients of lift and drag performed in Appendix A as well as the resulting Figure 2-2. From this figure, we can see that at the maximum lift angle of attack of approximately 0.7893 radians, the value of C_L is at its highest value of 3.3646, but the value of C_D is also very high at 3.3622. Although the vehicle is producing much lift at this angle of attack, it is also producing a lot of drag. This means that the vehicle is in turn slowing down, which referring back to the equations of lift and drag, indicates that the overall magnitudes of lift and drag will be decreasing with the velocity. If we take a look at the angle of attack which actually produced the longest flight at higher

34

altitudes, 0.3250 radians, we see that the corresponding values of C_L and C_D are 1.199 and 0.6583 respectively. Therefore, even though the C_L value is over 50% less, the C_D value is 500% less. The vehicle is able to maintain a high velocity and therefore a high lift for significantly longer periods, resulting in a longer trajectory in terms of time and distance.

Now that we have the shortest and longest trajectory with respect to angle of attack, we will look at cases with different initial conditions. The results of the DESIGN run with the angle of attack and roll set to 0.325 and 0.5 respectively is shown in Figures 5-13 through 5-16 (Case 3). When compared with Figures 5-9 through 5-12 where the roll was set to 0 radians, these graphs show a trajectory with the same shape and about 20% shorter range and time. When we look at graph 5-17 we see that the extra distance missing in downrange is translated into about 3500 km of crossrange.
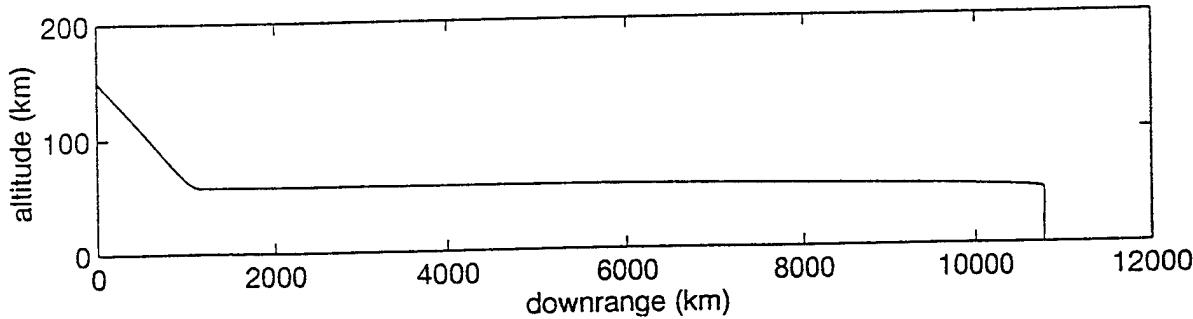
Figure 5-13 Case 3: Altitude vs Range
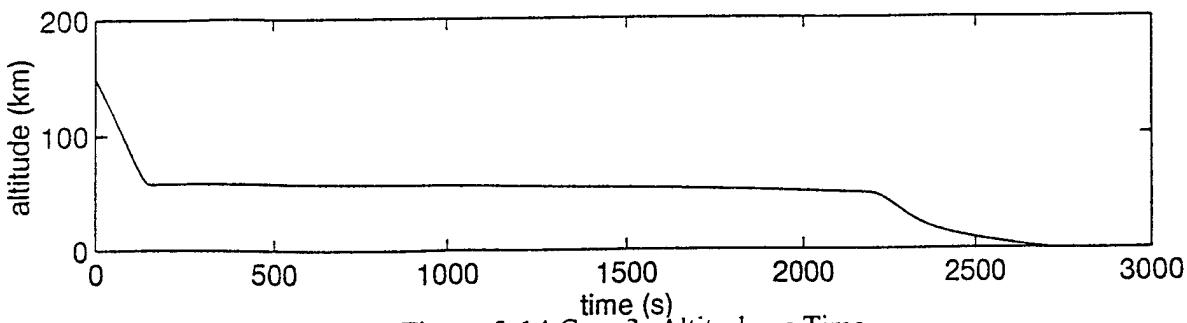
Figure 5-14 Case 3: Altitude vs Time
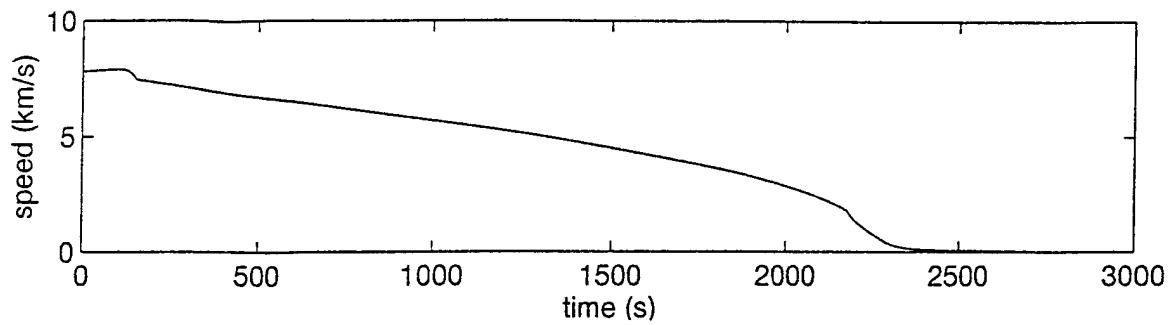
Figure 5-15 Case 3: Speed vs Time
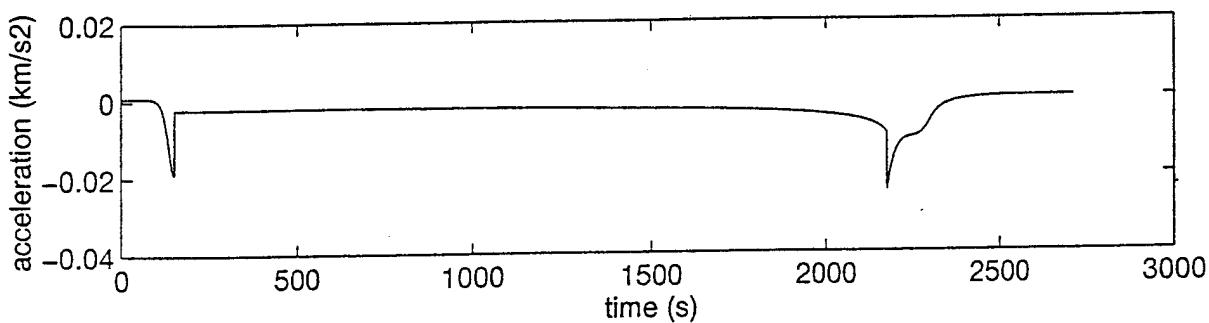
Figure 5-16 Case 3: Acceleration vs Time
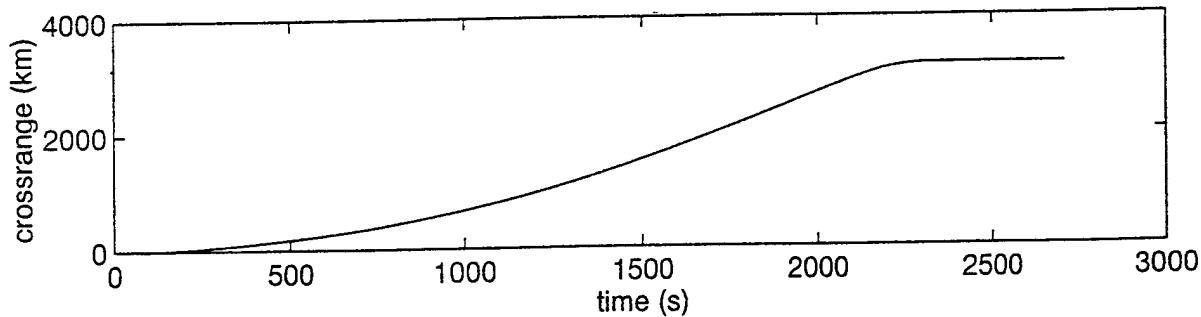
Figure 5-17 Case 3: Crossrange vs Time

In order to fully test the control algorithm, we want to look at two more extreme trajectories. The first one, with DESIGN results shown in Figures 5-18 through 5-21, has the angle of attack set at a very high value of 1.5, with the roll again set at zero (Case 4).

From these results, we can see that while there is some lift generated at this angle of attack, the drag is also very high, therefore, the trajectory, while longer than the ballistic trajectory, is significantly shorter than the trajectories with a lower angle of attack.
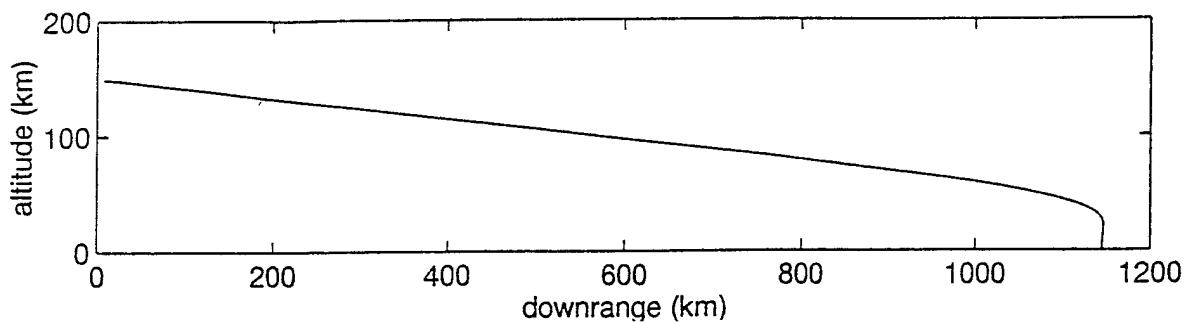
Figure 5-18 Case 4: Altitude vs Range
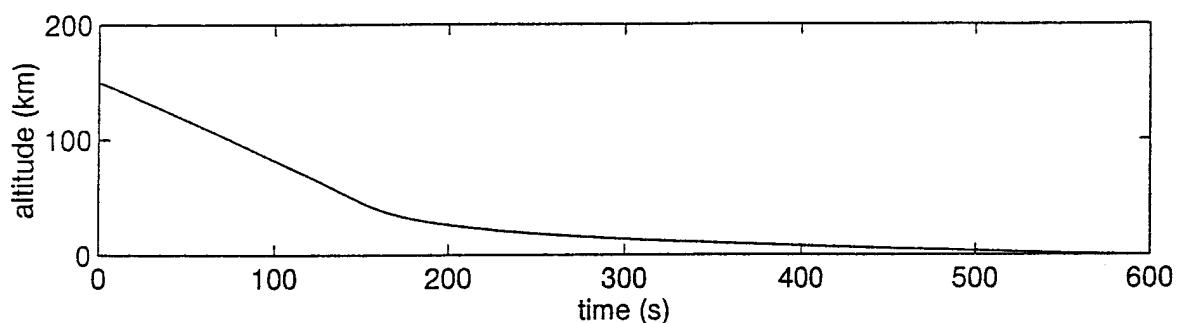
Figure 5-19 Case 4: Altitude vs Time
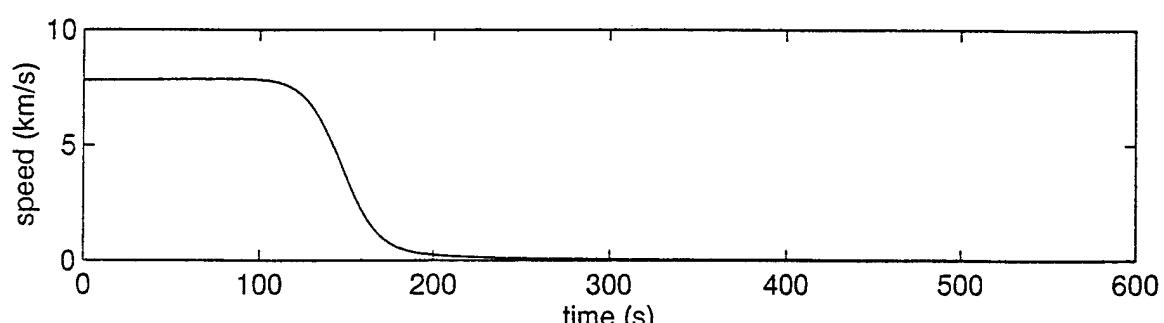
Figure 5-20 Case 4: Speed vs Time
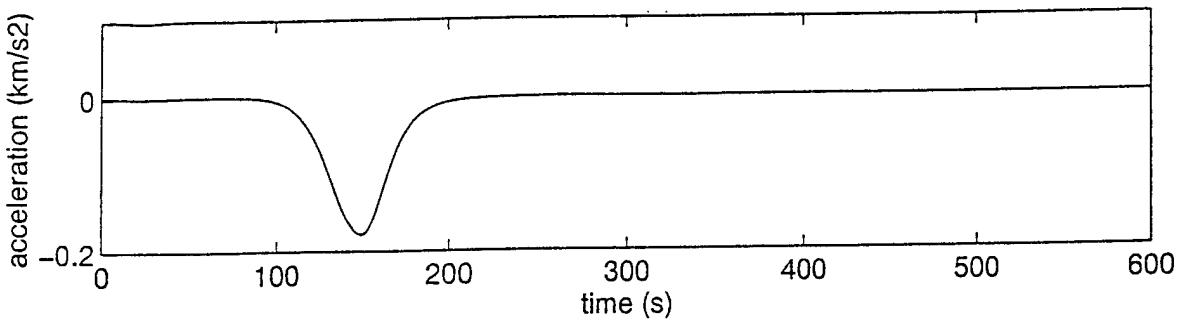
Figure 5-21 Case 4: Acceleration vs Time

The last trajectory we will examine is one with a roll of 0.5 radians and zero angle of attack (Case 5). As we can see from Figures 5-22 through 5-25, this trajectory is almost identical to the ballistic trajectory. The only difference can be seen in Figure 5-26, where the very slight crossrange can be seen. This crossrange value is equal to about 150 nanometers, which can be attributed to round off error in the integration.
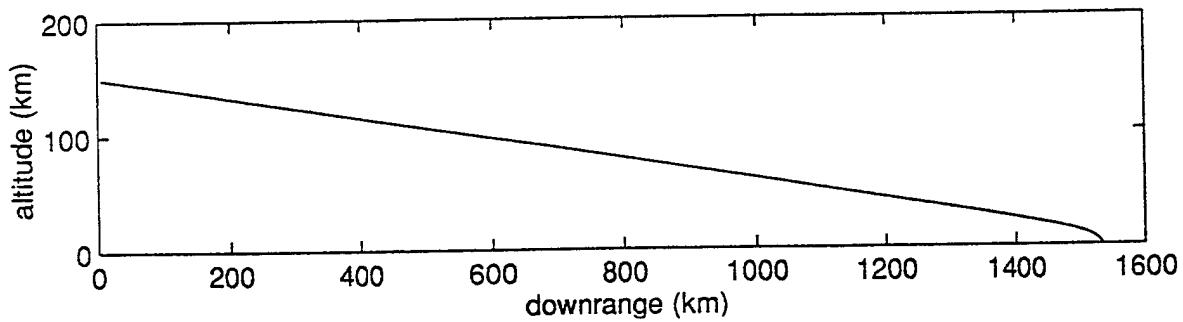
Figure 5-22 Case 5: Altitude vs Range
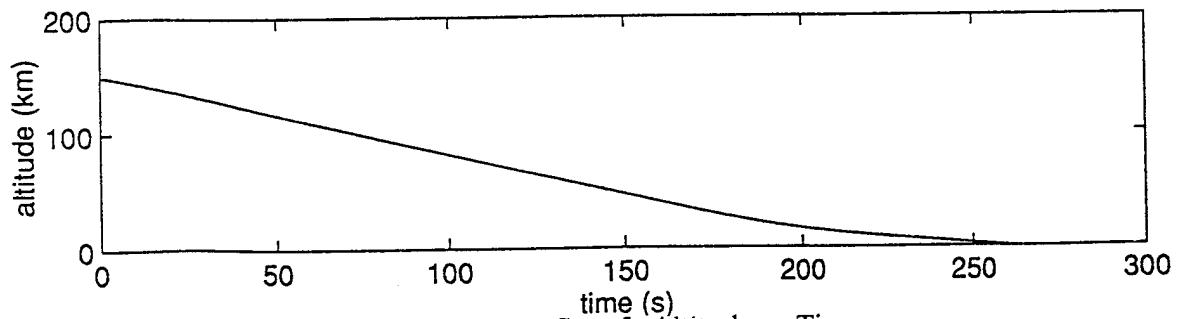
Figure 5-23 Case 5: Altitude vs Time

38

Figure 5-24 Case 5: Speed vs Time

Figure 5-25 Case 5: Acceleration vs Time

Figure 5-26 Case 5: Crossrange vs Time
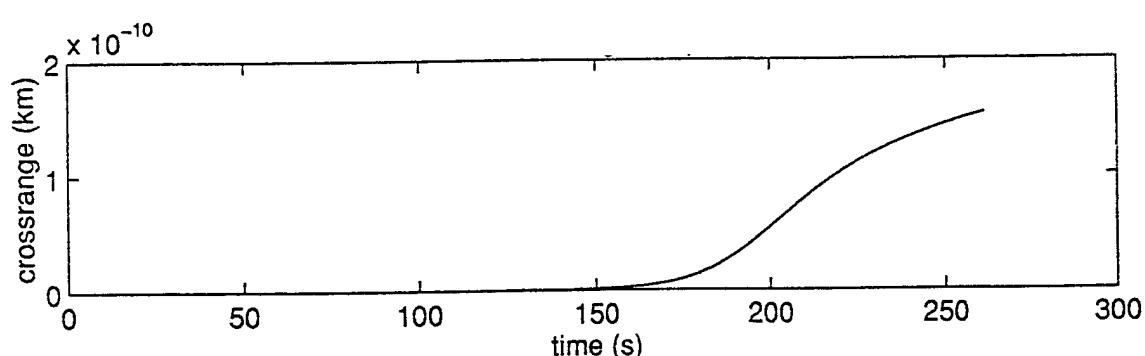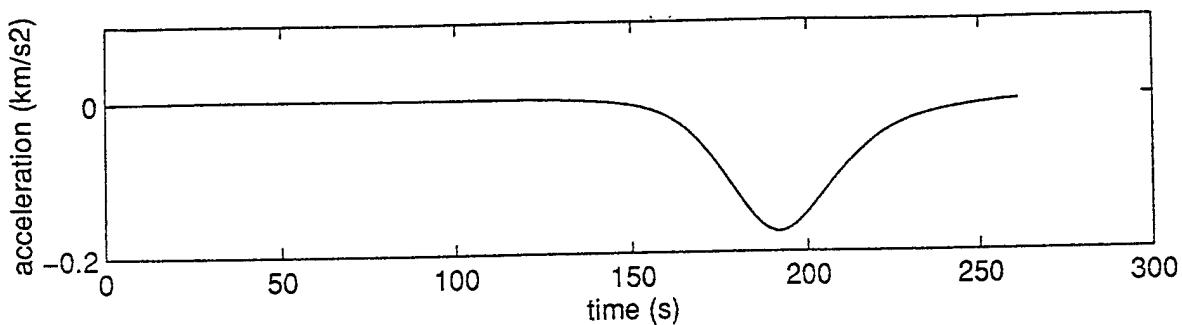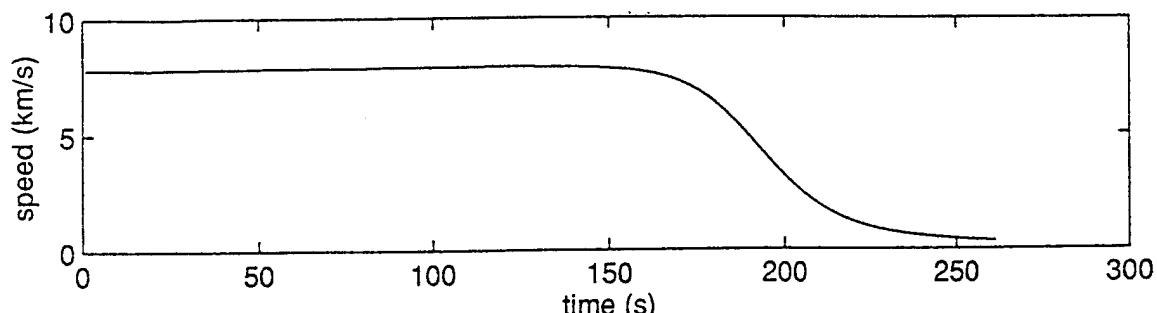
. Since, in this case, we have roll with no angle of attack and we are using a cone to model our vehicle, we do not expect to get any change in the trajectory by simply varying the roll.

The summary of all the cases and their basic trajectory characteristics is listed below in Table 5-2. As predicted, cases 2 and 3 are the better trajectories, in terms of length of flight and deceleration experienced during reentry. Operationally, the large downrange values allow for correction in the event of an error in the initial conditions of the trajectory. By initially planning on overshooting the launch pad, we are able to correct for any errors in our trajectory entry point conditions by simply adjusting the control variables in the middle of the reentry. Therefore if no errors are made, we are able to cut the trajectory length down to the required value. However, if errors do occur, we can simply make use of the planned overshoot to get the vehicle to the landing pad. Cases 1, 4 and 5 represent the other extreme trajectories which allow us to further test the control algorithm.

| Case	Initial Angle of Attack (rad)	Initial Roll (rad)	Time of Trajectory (sec)	Downrange (km)	Crossrange (km)	Maximum Deceleration (km/s^2)
1	0.0000	0.0	261.16	1535	0	0.173
2	0.3250	0.0	3090.91	13310	0	0.021
3	0.3250	0.5	2721.15	10777	3664	0.024
4	1.5000	0.0	596.15	1150	0	0.175
5	0.0000	0.5	261.54	1533	1.53e-10	0.173

Table 5-2 Trajectory Characteristics

5.2 Trajectory Control   Now that the test cases have been set up using DESIGN, we can begin to implement the control algorithm by running FIRST. As discussed earlier, this program iterates through the given trajectory and determines the open loop Lyapunov exponents and principal dynamical directions for that case's initial conditions. Table 5-3

contains the open loop Lyapunov exponents from the results of the FIRST runs for each case.

	CASE 1	CASE 2	CASE 3	CASE 4	CASE 5
Initial Angle of Attack	0.0	0.325	0.325	1.5	0.0
Initial Roll	0.0	0.0	0.5	0.0	0.5
Lyapunov Exponents	-26.3763	-1.9174	-0.0072	-11.9515	-3.6924
	-7.7822	-0.0394	24.1390	-10.5145	-1.1031
	0.0000	33.4578	25.2178	-0.0159	0.0000
	0.0000	40.7560	32.7295	0.0000	0.0000
	0.0699	41.3092	32.9773	0.0091	0.0098
	13.6055	50.4748	40.6461	4.9930	1.8985

Table 5-3 Open Loop Lyapunov Exponents

Looking at the Lyapunov exponents, we can see that all the trajectories are unstable, that is, they have unstable, positive, Lyapunov exponents. We can also see that they are all chaotic. For our purposes, we will define a chaotic system as one that has both positive and negative Lyapunov exponents. The presence of positive exponents means that we cannot fully predict where the system will be at some future time. This means that we will have problems controlling longer trajectories.

Due to the negative exponents, we also cannot determine where the system was in the past. The reason for the presence of large negative exponents in Case 4 can be seen in Figures 5-18 and 5-19. From these graphs we can see that for this trajectory the vehicle accomplishes all its downrange flight in roughly the first three minutes of the trajectory. For the remaining 6.5 minutes, the vehicle is basically falling out of the sky. This convergence of velocity vectors to the vehicle's terminal velocity is what causes the presence of the highly negative exponents. All the cases' trajectories have this

convergence of velocity vectors, but the differing lengths of the trajectories will dictate how much of a problem results from the convergence.

The problem with large negative open loop Lyapunov exponents can be found in the following development. We will start with the adjoint of the open loop Φ_λ equation as follows.

$$\dot{\Phi}_\lambda = -A^T \Phi_\lambda$$

Using the derivative of the identity matrix $I = \Phi_x \Phi_x^{-1}$,

$$\frac{d}{dt}(I) = \dot{\Phi}_x \Phi_x^{-1} + \Phi_x \frac{d}{dt}\left(\Phi_x^{-1}\right) = 0,$$

and the equation of variation, $\dot{\Phi}_x = A\Phi_x$, we get the following equation.

$$\Phi_x \left(\dot{\Phi}_x^{-1}\right) = -AI = -A$$

by matrix algebra this reduces to

$$\left(\dot{\Phi}_x^{-1}\right)^T = -A^T \left(\Phi_x^{-1}\right)^T$$

when combining this with the adjoint equation listed above, we get the following significant relationship where C is a constant.

$$\Phi_\lambda = C\left(\Phi_{x,OL}^{-1}\right)^T$$

This means that large negative open loop Φ_x Lyapunov exponents equate to large positive Φ_λ Lyapunov exponents, which result in the Φ_λ matrix blowing up. Therefore, while negative exponents are usually considered favorable, this algorithm cannot handle very large negative Lyapunov exponents for long periods of time.

Because Cases 2 and 3 have very large positive unstable exponents, we could expect to have some trouble controlling them for large lengths of time since the system will react proportional to e^{Lt} where L is the Lyapunov exponent. We could also predict some difficulties with Case 1 since it has both highly negative and positive exponents. However, since this is the shortest trajectory, we may avoid significant problems. The open loop dynamical direction vectors **u** and **v** for each of the cases can be found in Appendix J.

We now want to use the control algorithm to stabilize the trajectories. We will make runs with BVP and specify that the closed loop dynamical direction vectors **u** and **v** will be the same as their open loop values and the closed loop Lyapunov exponents will be arbitrarily chosen as follows.

<u>**Desired Closed Loop Lyapunov Exponents**</u>
-0.1000
-0.2000
-0.3000
-0.4000
-0.5000
-0.6000

The closed loop Lyapunov exponents resulting from the BVP runs for the different cases are listed in Table 5-4.

It is obvious from these results that the algorithm performs very well on the first and last cases, and very poorly on the other three cases. Cases 1 and 5 actually produce Lyapunov exponents that agree with the desired values to the seventh decimal place. Therefore we can say that for all intents and purposes, the problem of stabilizing the

43

trajectories in these two cases has been solved. The closed loop dynamical direction

vectors, **u** and **v**, can be found in Appendix K.

	CASE 1	CASE 2	CASE 3	CASE 4	CASE 5
Initial Angle of Attack	0.0	0.325	0.325	1.5	0.0
Initial Roll	0.0	0.0	0.5	0.0	0.5
Lyapunov Exponents	-0.09999	50.84818	41.69156	9.02201	-0.10000
	-0.20000	49.74232	39.80656	4.23818	-0.19999
	-0.30000	42.82911	33.84590	0.00415	-0.30000
	-0.40000	41.98179	31.43286	0.00001	-0.39999
	-0.49999	34.29443	25.58373	-3.84421	-0.50000
	-0.59999	-0.59297	-0.00735	-7.10920	-0.59999

Table 5-4 Closed Loop Lyapunov Exponents

We must, however, look at the cases for which the control algorithm was unable

to accomplish the desired Lyapunov exponent values and determine the reasons why the

algorithm was unsuccessful. If we look closely at Figures 5-18 and 5-19, we can see a

possible reason for the inability of the algorithm to set the desired exponents in case 4. As

discussed earlier, in Figure 5-19 we see that the altitude decreases to a value of

approximately 36 km at a downrange value of about 1150 km at which point the vehicle

basically drops out of the sky. While this is never a good thing for a launch vehicle to do,

we can allow this kind of trajectory for now, since we are testing the algorithm. If this

were an actual trajectory being flown by a launch vehicle, the necessary adjustments could

be made. While the vehicle reaches this altitude near the end of its trajectory in terms of

range, Figure 5-18 shows that it only takes about 200 seconds to reach this altitude. This

means that roughly the last 6.5 minutes of the trajectory is spent in freefall, which for our

purposes, is not worth trying to control. Therefore, if we cut down the time of the

trajectory arc that we are trying to control to about 200 seconds, the algorithm should be

able to control it. We can see from Case 4 in Table 5-5 that this is true. For the important (non-freefall) portion of the trajectory, we are able to determine the closed loop Lyapunov exponents and dynamical direction vectors (see Appendix K).

Now we must focus on Cases 2 and 3. There is one major difference which is initially apparent between Cases 2 and 3 and the other three. This difference can be seen in Table 5-2 in the total time of the trajectories. Cases 2 and 3 have times from 5 to 10 times greater than Cases 1, 4, and 5. To understand the reason why these longer trajectories may cause problems, we must look back at our development of the boundary value problem in Chapter 3.

In the development of the algorithm in Chapter 3, we see that the dual sweep method requires that we sweep the S_f matrix back through time to get the S_0 matrix and then the $\lambda_0(t)$ values. We then sweep forward to get the state and λ values throughout the trajectory. Since the trajectories that had problems are the longer ones, it appears that our earlier assumption, that the trajectories we were evaluating were short enough to be performed in one piece, was invalid. Recall that finite integrations are needed for all chaotic trajectories. To determine whether this was our problem, we can simply cut down the length of the trajectory that we are attempting to control and see if that allows us to control it. In order to accomplish this, we use DESIGN, but limit the maximum time to a length of the trajectory we think is controllable. After testing, it becomes apparent that the algorithm can handle initial trajectory arcs up to about 1.0 TU or 806 seconds for cases 2 and 3. Table 5-5 contains the open and closed loop Lyapunov exponents for cases 2 and 3 for these shortened trajectory arcs. Recall the results from Case 4 are also

included even though we shortened that case's trajectory for a different reason. The closed loop dynamical direction vectors for these arc are also in Appendix K.

We can see that the desired closed loop dynamical direction vectors, $\mathbf{u}$ and $\mathbf{v}$, for all the cases match to within a couple of significant figures. The only apparent problem is the fact that in some cases (ie Case 1 $\mathbf{u}_4$ and $\mathbf{v}_4$) the entire vector is the negative of the specified desired closed loop value. No information is lost here, but the vector is set up in a left handed frame instead of a right handed one. This problem can be traced to the method in which the Φ matrix is decomposed in the subroutine SVDCMP.

	CASE 2 0.0-1.0 TU		CASE 3 0.0-1.0 TU		Case 4 0.0-0.25 TU	
Initial Angle of Attack	0.325		0.325		1.5	
Initial Roll	0.0		0.5		0.0	
Lyapunov Exponents	Open	Closed	Open	Closed	Open	Closed
	-9.7556	-0.1076	-9.9592	-0.1101	-34.134	-0.0984
	-0.5318	-0.2000	-0.5532	-0.2000	-22.803	-0.2000
	-0.0959	-0.3000	-0.1191	-0.3000	0.0002	-0.3000
	0.0880	-0.4000	0.0887	-0.4000	0.0531	-0.4000
	1.5695	-0.5000	1.4576	-0.5000	0.09130	-0.5000
	8.3264	-0.5999	8.6196	-0.5999	21.9392	-0.6000

Table 5-5 Open and Closed Loop Lyapunov Exponents for Limited Trajectory Arc

For Cases 2 and 3, we can control the rest of the trajectory in small arcs that the program can handle. We must then paste together the short arcs of the trajectories so that by controlling the separate pieces, we are in effect controlling the whole reentry trajectory. To do this correctly, we must review what the $\mathbf{u}$ and $\mathbf{v}$ vectors represent. Since we want the control to be smooth throughout the entire trajectory, we must set the $\mathbf{v}$ vector of the second arc equal to the $\mathbf{u}$ vector of the first arc and so on throughout the trajectory as

seen in Figure 5-27. Up to this point, we have simply set the closed loop dynamical direction vectors equal to their open loop values; but since the control algorithm allows us to set both the closed loop Lyapunov exponents and dynamical direction vectors, this should not pose a problem.
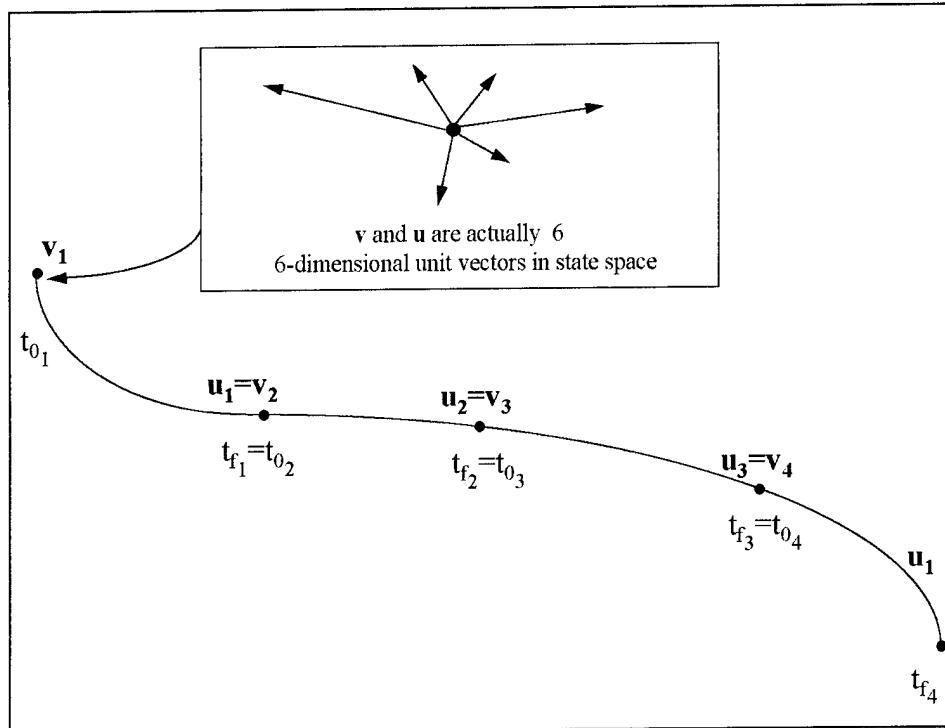
Figure 5-27 Piecemeal Trajectory

After attempting to obtain the remaining portions of the trajectory for cases 2 and 3, we found that as we get closer to the impact point, we are able to control only 5 of the 6 Lyapunov exponents. This is most likely due to the same problem encountered in Case 4. The convergence of the velocity vectors is simply too swift in this region for the algorithm to handle.

For each of these 5 cases, the gain matrix, which will be used in the reentry vehicle to implement the control of the trajectory, has been printed to a file at every iteration of

For each of these 5 cases, the gain matrix, which will be used in the reentry vehicle to implement the control of the trajectory, has been printed to a file at every iteration of the trajectory, along with the time and the state vector at that time. To ensure that these gains can be implemented in the real world vehicle, we will graph the individual components of the gain matrix vs time. A plot of this type for Case 1 can be seen in Figure 5-28.
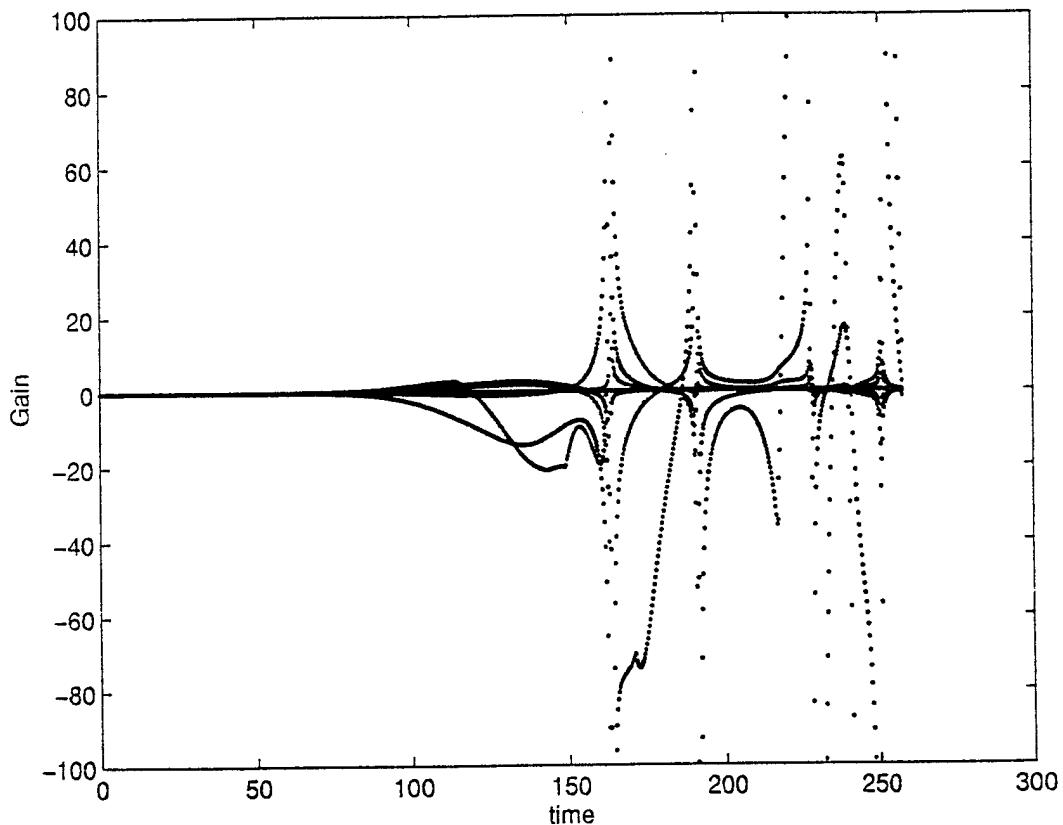
Figure 5-28 Case 1: Gain Plot

There seem to be several points which require very high gain to stabilize them. We can see from Figure 5-4 that these seem to occur at the point in the trajectory where the vehicle is going through a sizable deceleration due to aerodynamic forces. It would make sense that at this point the vehicle would be hard to control. It appears as though these

problem points may go to a gain value of infinity which would signify that although the control algorithm was able to set the Lyapunov exponents, it required an unrealistic, unachievable amount of control by the mechanical systems of the vehicle to accomplish it. Therefore, while the algorithm is able to specify stable Lyapunov exponents, the real world system would not be able to accomplish them.

Figures 5-29 through 5-32 show the gain plots for the other 4 cases. We see that these are very similar to the plot for Case 1. Looking at acceleration vs time plots for these cases, we can see that most of the problem points seem to appear in the area of maximum deceleration in the trajectory. One possible method for eliminating these spikes of infinite gain is to choose the stable Lyapunov exponents such that the control algorithm is able to accomplish the required trajectory without resorting to infinite gain. Despite numerous attempts, we were unable to choose Lyapunov exponents which allowed a finite gain at all points. We were, however, able to change the position and number of infinite spikes.

Figures 5-33 through 5-35 are gain plots of the shortened trajectory of Case 2 with the desired closed loop Lyapunov exponents changed. Notice in Figure-33, where the Lyapunov exponents were all set to zero, there are only three spikes, with one being at the very end of the trajectory. All other times have very reasonable gains. Figure 5-34, which had Lyapunov exponents of -1, -2, -3, -4, -5, and -6, has the same number of spikes, but the two mid-trajectory spikes have moved much closer together. Figure 5-34, where the Lyapunov exponents are all set to -100.0, has only two infinite spikes, but the gain values towards the end of the trajectory get very large long before they actually go to infinity.

The fact that we can alter the number and position of these infinite spikes leads to the conclusion that a combination which produces no spikes should exist, even though we were unable to discover it.
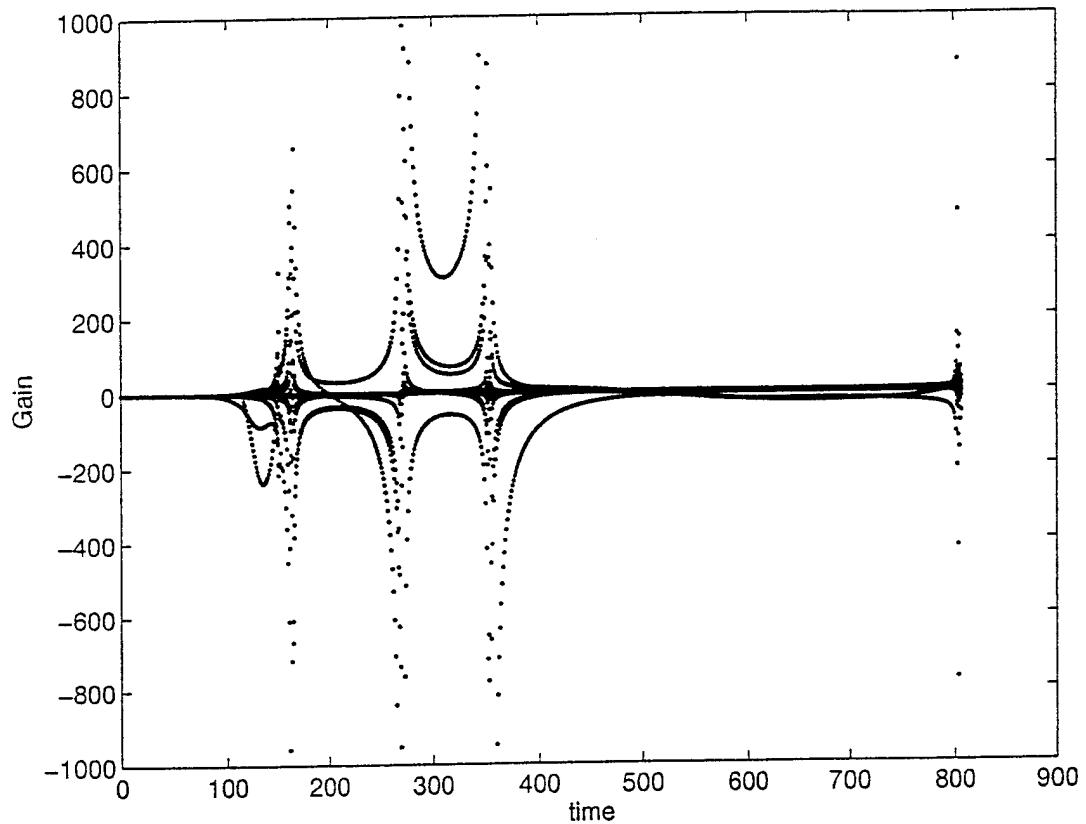
Figure 5-29 Case 2 (0-1.0 TU): Gain Plot
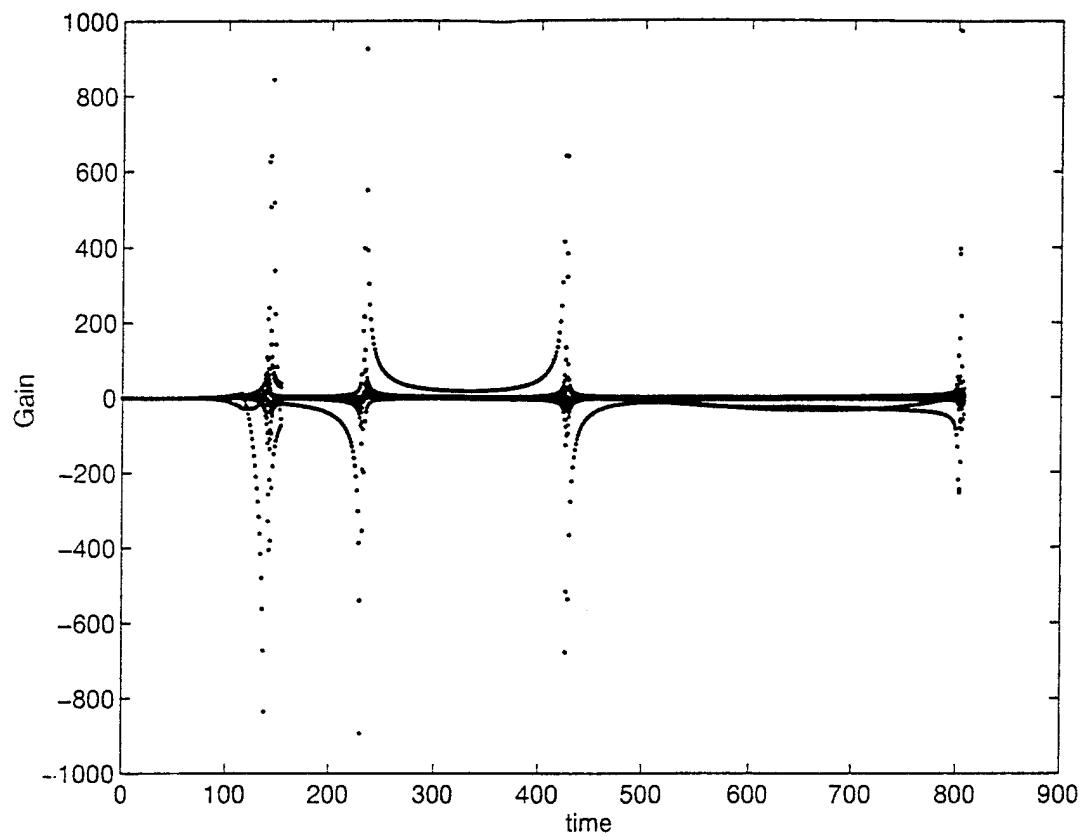
Figure 5-30 Case 3 (0-1.0 TU): Gain Plot
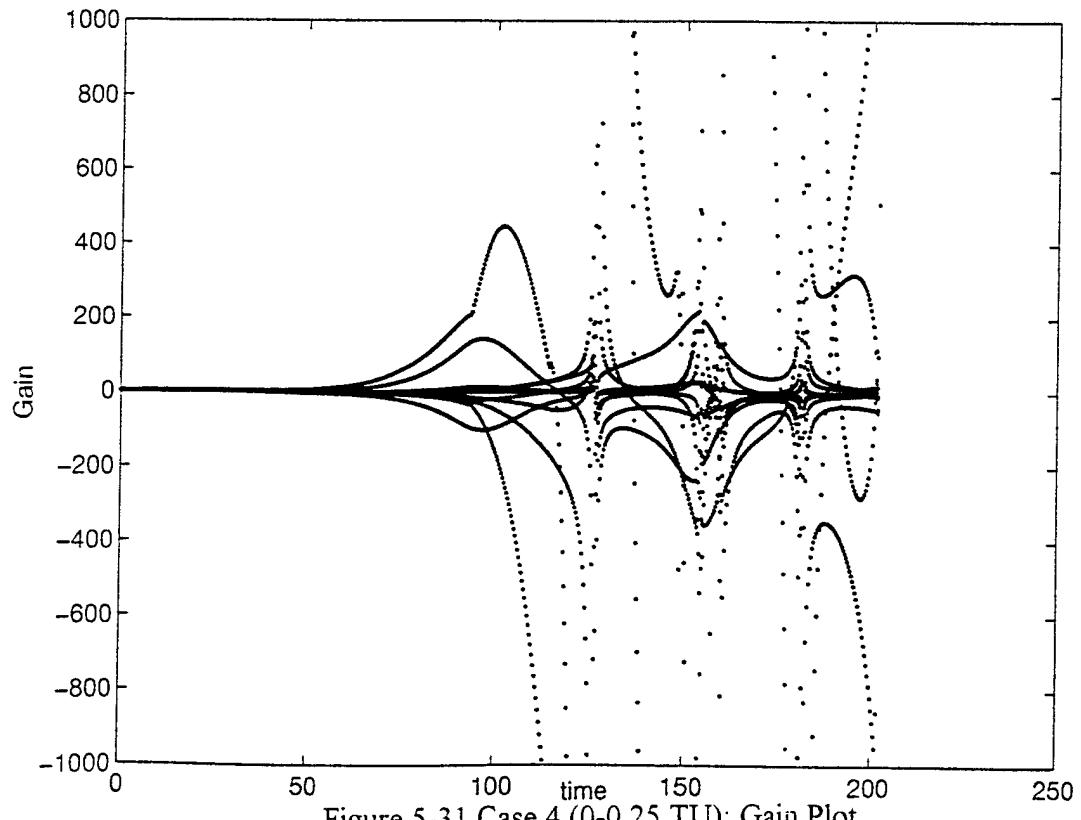
Figure 5-31 Case 4 (0-0.25 TU): Gain Plot
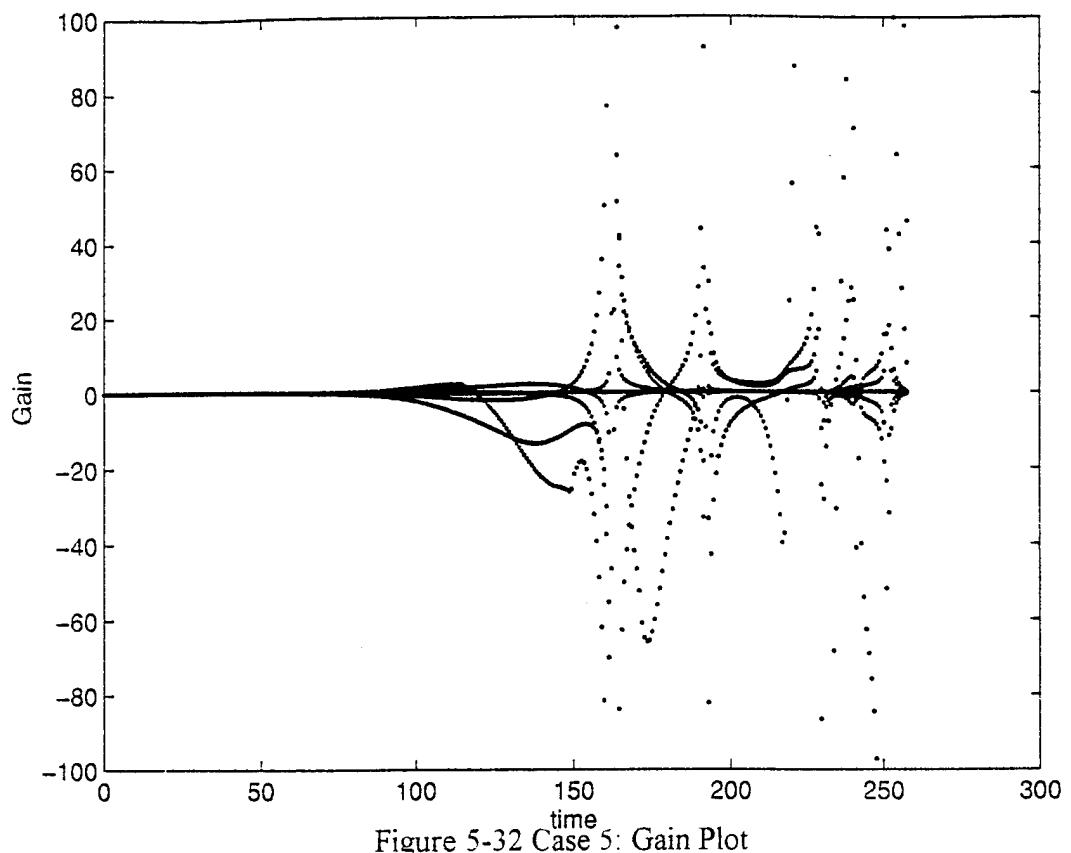
Figure 5-32 Case 5: Gain Plot
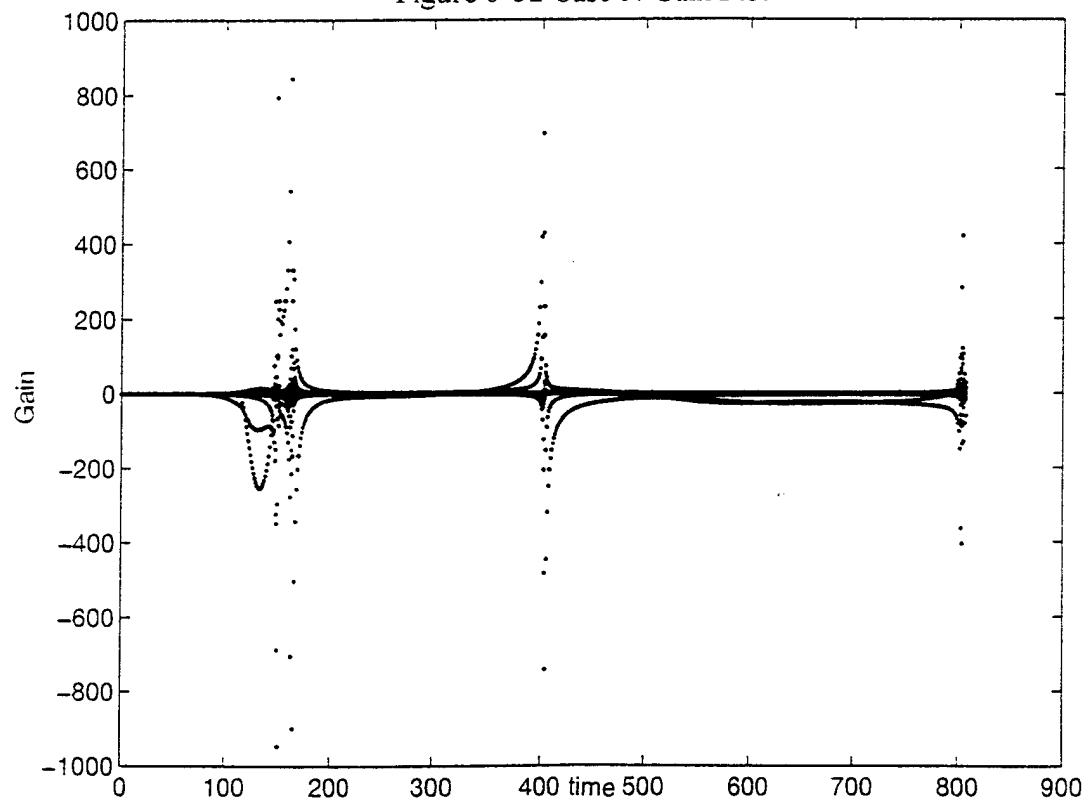
Figure 5-33 Case 2 (0-1.0 TU): Gain Plot with Lyapunov exponents = 0.0
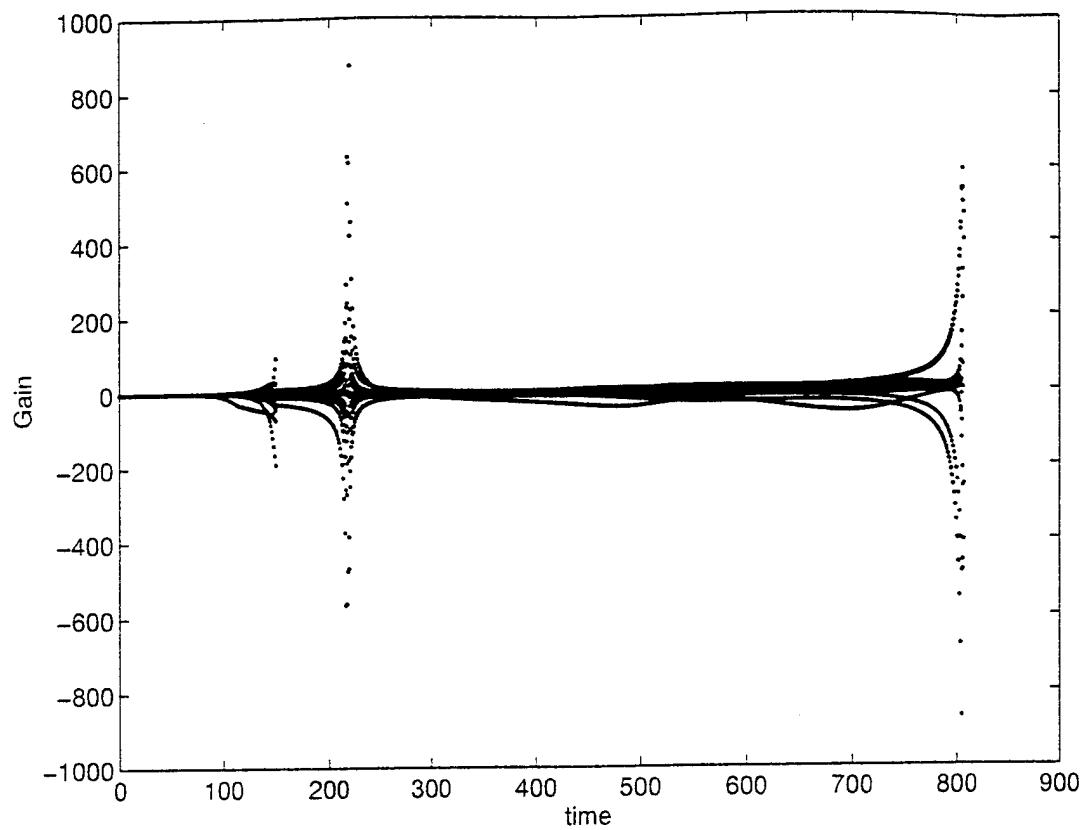
Figure 5-34 Case 2 (0-1.0 TU): Gain Plot with Lyapunov exponents = -1, -2, -3, -4, -5, -6
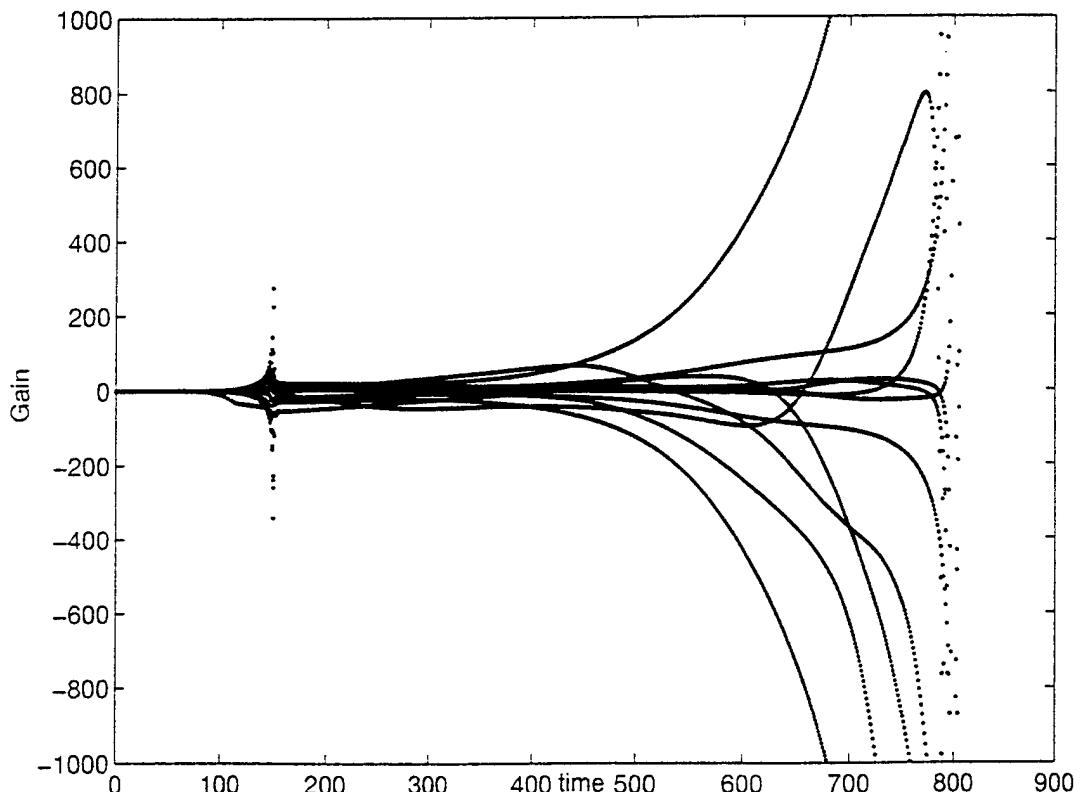
Figure 5-35 Case 2 (0-1.0 TU): Gain Plot with Lyapunov exponents = -100.0

53

VI. Conclusions and Recommendations

6.1 Conclusions.   Having looked at five cases and the control algorithm's ability to control them, there are several conclusions we can draw. First, we must realize that these test cases do not necessarily correspond to any operationally useful trajectories that a Delta Clipper-like vehicle would fly. They were chosen because they had characteristics which would challenge the bounds at which the algorithm performs. The initial control law modeled in the vehicle was chosen to keep the vehicle at high altitudes for as long as possible given the initial conditions. This may or may not be the desired objective of a given reentry. Therefore, while only two of the cases were controlled in their entirety, we can still claim to have successfully proven the strengths and weaknesses of Wiesel's algorithm.

Cases 1 and 5 were handled completely successfully by the algorithm. Cases 2 through 4 are longer trajectories which have swift convergence of the velocity vectors in the middle of the trajectory as the aerodynamic forces strongly affect the vehicle. While this is a shortfall in algorithm performance, the inability of the algorithm to specify all stable Lyapunov exponents in these cases is more based on the inherent characteristics of the trajectories themselves than the robustness of the control algorithm. From the results of the previous section it is clear that the algorithm can handle pole placement for large arcs, if not entire trajectories for most reentry situations. Another problem became apparent when comparing the desired and achieved closed loop dynamical direction

vectors. Certain vectors ended up being the negative of their desired values. While no information is lost, this is still something that needs to be addressed.

Another weakness was discovered in the gain matrices produced by the program. For randomly chosen stable exponents, the gain matrix produced by the algorithm had several points which approached infinity. This is obviously a problem since no real world system would be able to implement such gain. While changing the desired Lyapunov exponents affected the number and location of these infinite spikes, we were unable to totally eliminate them. The ability to affect the singularities by changing the desired Lyapunov exponents leads to the conclusion that choosing the correct exponents would allow the gain matrix to be finite.

Still, despite the weaknesses stated above, the usefulness of this algorithm should not be overlooked. The ability to place the poles and dynamical direction vectors of a given chaotic time dependent system without modeling it as a constant coefficient system is invaluable. Due to the nature of chaotic systems, there may be some limits on the length of time a given system can be controlled. This will tend to be a problem for any control algorithm dealing with time dependent chaotic systems. Wiesel's method gives us the ability to do realistic control for long periods of time.

6.2 Recommendations   There are several areas which rate further research before Wiesel's control algorithm can be termed a complete success. The research in this paper concentrated on a Delta-Clipper like vehicle with two control variables and a given control law. A more vigorous test of the algorithm would be to vary the vehicle's control law for

given initial conditions and evaluate how the algorithm handles the different trajectories. Another possible test would be to increase the number of control variables and vary the control matrix away from the identity matrix which was used in this research.

More work should be done in determining the exact reasons for and quantifying the boundaries of the inability of the algorithm to handle long arcs of trajectory. While we discussed the dual sweep algorithm and the difficulties it poses, the actual limits of the Linear Quadratic Regulator as well as possible alternative methods need to be explored in depth.

As stated earlier, the problem with the SVDCMP subroutine, which returned the negative of the **u** and **v** vectors in a seemingly random pattern, needs to be evaluated further. This is a situation which can be worked around in the short term since the resulting values are simply the negative of the desired vectors. This may well be a problem which can be solved by implementing a different decomposition routine, but the matter needs to be examined.

Finally, the problems with the gain matrix discussed above need to be more thoroughly examined. Other possible methods for calculating the gain matrix need to be evaluated as do the ranges of acceptable stable exponents. More work needs to be done to see if it is possible to choose stable exponents that actually give finite gain at all points. If we are eventually able to iterate through exponents and pick ones which do not cause infinite spikes, we should be able to discover an algorithm which takes this into account when calculating the gain matrix. At the very least, there should be a method of determining, at the outset of the problem, which Lyapunov exponents would tend to move us closer to a continuously finite gain matrix vs those that would move us away from one.

While, overall, Wiesel's algorithm is both very powerful and very useful, addressing these issues could lead to a more full proof method which has the potential to gain acceptance throughout the control community.

Bibliography

1. Bate, Roger R., Donald D. Mueller, and Jerry E. White, <u>Fundamentals of Astrodynamics</u>. New York, Dover Publications Inc. 1971.

2. Breakwell, J.V., A. Kamel, and M.J. Ratner, "Stationkeping for a Translunar Communications Station," *Celestial Mechanics*, Vol. 10, 1974, pp357-373

3. Bryson, Arthur E., Jr and Yu-Chi Ho, <u>Applied Optimal Control: Optimization, Estimation and Control</u>, New York, John Wiley and Sons, 1975 pp148-152

4. Copper, John A. "Future Single-Stage Rockets: Reusable and Reliable" *Aerospace America*. February 1994. pp18-21

5. Copper, John A. "Single Stage Rocket Concept Selection and Design" *AIAA Space Programs and Technologies Conference*. March 24-27, 1992 Paper 92-1383

6. Eshbach, Ovid W. and Mott Souders, ed. <u>Handbook of Engineering Fundamentals</u>. New York, John Wiley & Sons, 1975.

7 Etter D.M. <u>Structured FORTRAN 77 for Engineers and Scientists</u>, Reading, Massachusetts, Benjamin/Cummings Publishing Company Inc. 1983.

8. Gaubatz, William A. and Jess Sponable. "A Technology and Operations Assessment of Single Stage Rocket Technology Flight Test Program Results." AIAA 1993

9. Ladner, Pat and Jess Sponable. "Single-Stage-Rocket-Technology: Program Status and Opportunities."AIAA 1992

10. Regan, Frank J. and Satya M. Anandakrishnan. <u>Dynamics of Atmospheric Reentry</u>. Washington DC: American Institute of Aeronautics and Astronautics, Inc., 1993.

11. Vinh, Nguyen X., Adolf Busemann and Robert D. Culp, <u>Hypersonic and Planetary Entry Flight Mechanics</u>, Ann Arbor, University of Michigan Press, 1975

12. Wiesel, William E. and Robert A. Calico. "Control of Time-Periodic Systems." *Journal of Guidance Control and Dynamics*. Vol 7, No. 6, Nov - Dec 1984 pp671-676.

13. Wiesel, William E. "Full Stability Exponent Placement in Chaotic Systems." *Phys. Rev. E*, 1995, Preprint

14 Wiesel, William E. "Optimal Pole Placement in Time-Dependent Linear Systems." *Journal of Guidance Control and Dynamics*. v18, 1994, pp995-999.

APPENDIX A: Lift and Drag on a Cone

In order to determine the coefficients of lift and drag it will be necessary to model the vehicle. For our purposes, we will use a cone with and 8° half angle. While this is obviously not a perfect representation, Figure A-1 shows that it should be adequate for our purposes.

127 ft

8°

18 ft

18 ft

Vehicle Specifications
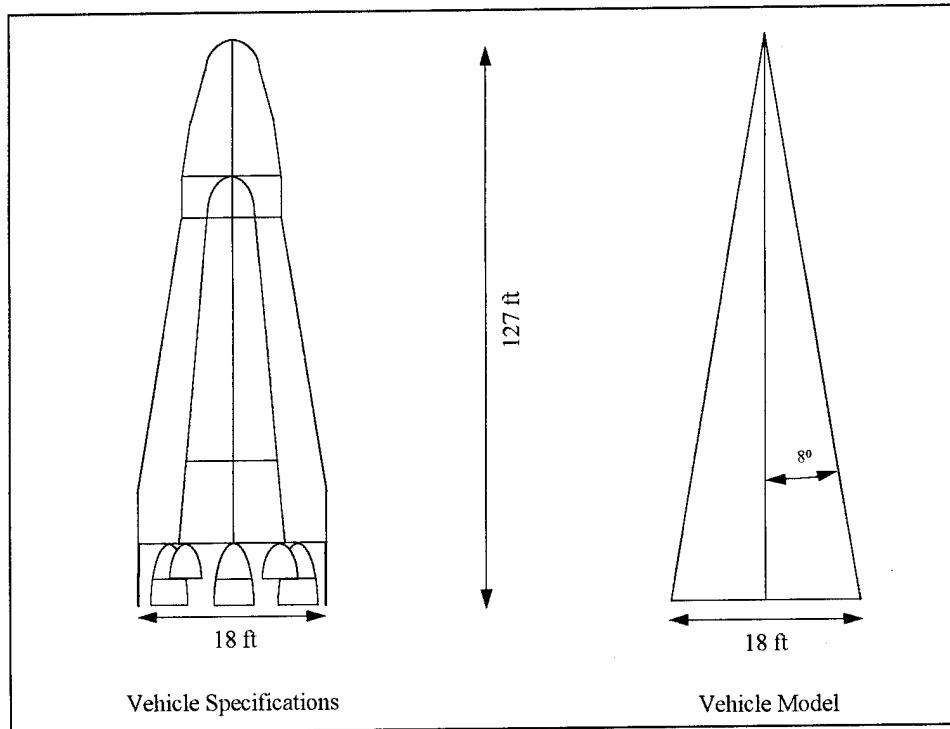
Vehicle Model

Figure A-1 Vehicle Aerodynamic Model

Now that we have determined a model, we must set up the coordinate frames we are going to use in our development. Figure A-2 shows the two main coordinate frames and some of the important variables we will use in our discussion. The velocity dependent coordinate frame will consist of a v_1 axis in the direction of the vehicle's velocity vector, a
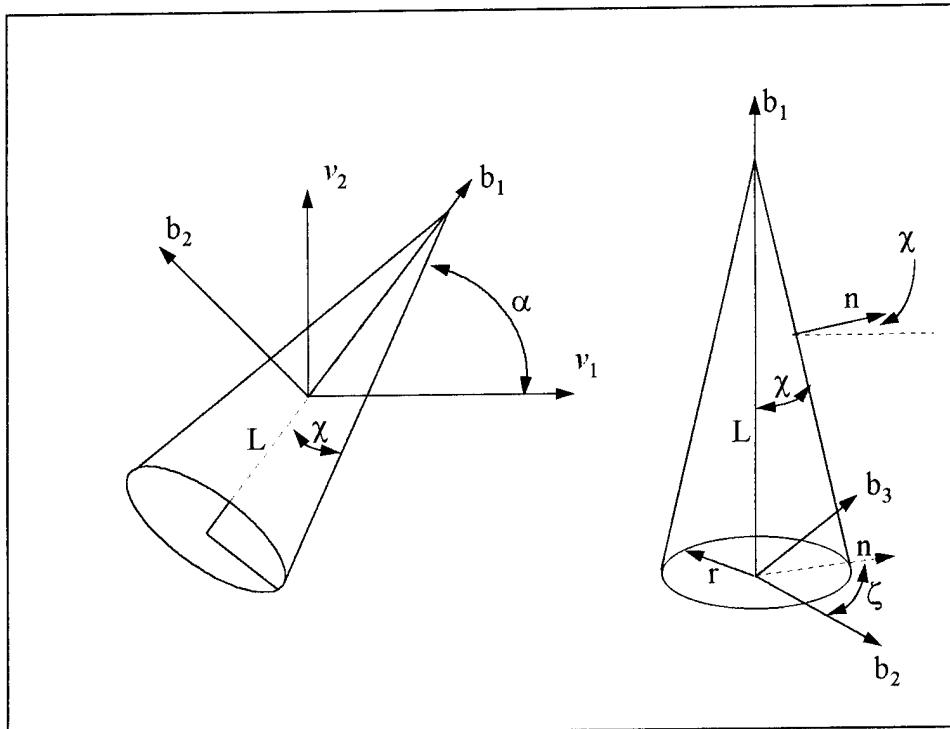
Figure A-2 Coordinate Frames and Important Variables

v_2 axis in line with the radius vector from the center of the earth and a v_3 axis completing

the right-handed system. The body centered coordinate frame will consist of a b_1 axis

along the vertical center line of the vehicle, with the b_2 and b_3 axes fixed to the base, b_3 in

the direction of the v_3 vector. We can now define some important values. The angle

between the v_1 vector and the b_1 vector will be the angle of attack of the vehicle, α, and

the angle between the local vertical plane (containing $\vec{r}$ and $\vec{V}$ vectors) and the

aerodynamic plane (containing $\vec{V}$ and $\vec{A}$) will be the roll, σ. These are our two control

variables. We will also define χ as the cone half angle, which ends up being the angle

between the b_2, b_3 plane and the surface normal vector. ζ will be defined as the angle

between the projection of the normal vector on the b_2, b_3 plane and the b_2 axis.

With these definitions accomplished, we are now able to write the equation of the

normal vector from the surface of the cone as follows:

$$\hat{n} = Sin(\chi)\hat{b}_1 - Cos(\chi)Cos(\zeta)\hat{b}_2 + Cos(\chi)Sin(\zeta)\hat{b}_3.$$

Using the following coordinate transform,

$$\hat{b}_1 = Cos(\alpha)\hat{v}_1 + Sin(\alpha)\hat{v}_2$$
$$\hat{b}_2 = -Sin(\alpha)\hat{v}_1 + Cos(\alpha)\hat{v}_2,$$
$$\hat{b}_3 = \hat{v}_3$$

we are able to determine the normal vector in terms of the velocity coordinate frame.

$$\hat{n} = \left(Sin(\chi)Cos(\alpha) + Cos(\chi)Cos(\zeta)Sin(\alpha)\right)\hat{v}_1$$
$$+ \left(Sin(\chi)Sin(\alpha) - Cos(\chi)Cos(\zeta)Cos(\alpha)\right)\hat{v}_2$$
$$+ \left(Cos(\chi)Sin(\zeta)\right)\hat{v}_3$$

Now if we look at an infinitesimally small surface element of the cone in Figure A-3, we
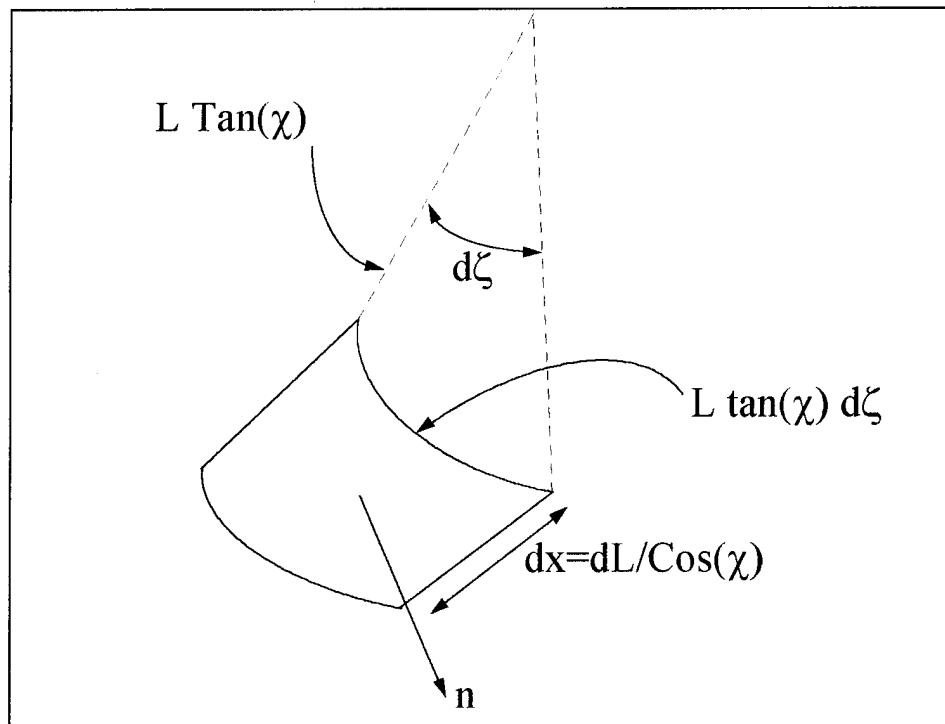
Figure A-3 Surface Element

can carry the derivation farther and determine the incremental area, such that

$$dS = \frac{L Tan(\chi)}{Cos(\chi)} dL d\zeta .$$

Then, if we picture the surface element flying through the reentry trajectory, we can see

that the mass intercepted over time dt is as follows

$$dm = dS \; \hat{n} \bullet \vec{V} \; dt \; \rho .$$

Now that we have the mass and the velocity, we will be able to calculate the change in

momentum. Looking at Figure A-4, we can see the value of the change in momentum,

Δp.
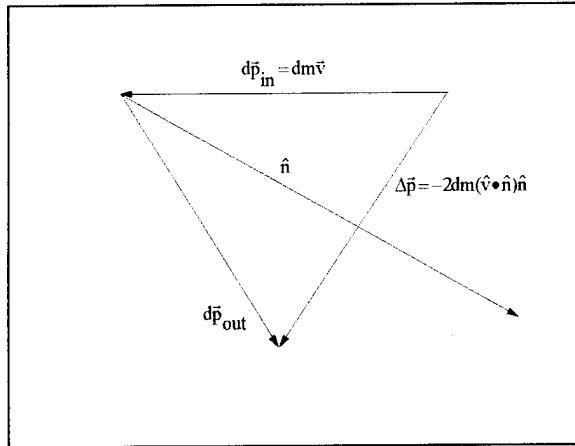
Figure A-4 Change in Momentum

Knowing this and assuming that the altitude and speed of the vehicle allow us to model the

air as a Newtonian fluid, we are able to use Newton's third law to calculate the

aerodynamic force, F_d in the following manner:

$$d\vec{F}_d = \frac{\Delta p}{dt} = -2(\hat{n} \bullet \vec{v})^2 \rho dS \hat{n} = -2(\hat{n} \bullet \vec{v})^2 \rho \frac{L Tan(\chi)}{Cos(\chi)} dL d\zeta \hat{n} ,$$

which leads to the following.

$$F_d = -2\int_0^L dL \int_{-\phi}^{+\phi} d\zeta \left(Sin(\chi)Cos(\alpha) + Cos(\chi)Cos(\zeta)Sin(\alpha)\right)^2 v^2 \rho$$

$$\times \frac{LTan(\chi)}{Cos(\chi)} \times \left\{ \begin{array}{c} (Sin(\chi)Cos(\alpha) + Cos(\chi)Cos(\zeta)Sin(\alpha))\hat{v}_1 \\ (Sin(\chi)Sin(\alpha) + Cos(\chi)Cos(\zeta)Cos(\alpha))\hat{v}_2 \\ (Cos(\chi)Sin(\alpha))\hat{v}_3 \end{array} \right\}$$

In this equation, the v_1 component is the drag component, the v_2 is the lift

component and the $v3$ component is the side force component. Based on Figure A-5, we

can see that the amount of surface area, while dependent on the angle of attack can not be

handled by a single integral. When the angle of attack gets larger than the cone half
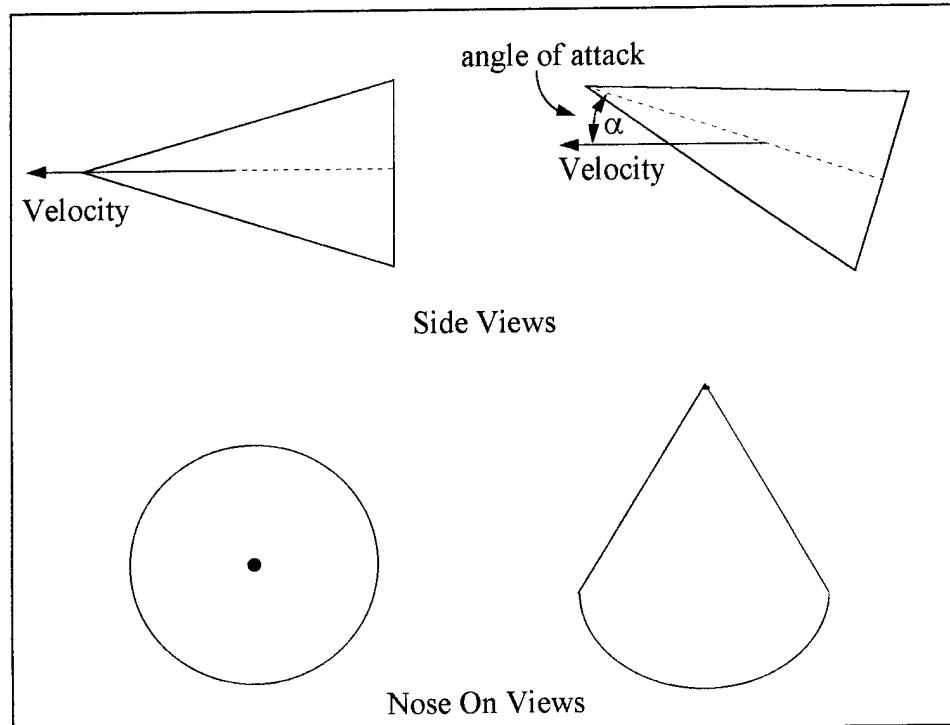
Figure A-5 Angle of Attack vs Surface Area

angle, the nose is now outside the original circular cross section. If we consider the

extreme where the normal vector to the surface and the velocity are perpendicular, we can

perform the following development.

$$n \bullet v = 0$$

$$Sin(\chi)Cos(\alpha) + Cos(\chi)Cos(\zeta)Sin(\alpha) = 0$$

$$Cos(\chi)Cos(\zeta)Sin(\alpha) = -Sin(\chi)Cos(\alpha)$$

$$Cos(\zeta) = -\frac{Sin(\chi)Cos(\alpha)}{Cos(\chi)Sin(\alpha)} = Tan(\chi)Ctn(\alpha)$$

This means that when the angle of attack is less than the half angle of the cone,

$Cos(\zeta) < -1$ and therefore the limits of ζ are $\pm\pi$. If $\alpha \geq \chi$ then $Cos(\zeta) > -1$ and

therefore $\zeta = Cos^{-1}(-Tan(\chi)Ctn(\alpha))$. From the text, we know the definition of Lift and

Drag, so referring back to Figure A-2 and the fact that the area of the base of the triangle

is $A = \pi r^2 = \pi L^2 Tan^2(\chi)$, results in the following equation.

$$\frac{C_D L^2}{A^2} = \frac{CD}{\pi Tan^2(\chi)}$$

By rearranging the equations of lift and drag and substituting them into the

previous equation, we get the following equations which can be used to determine the

64

coefficients of lift and drag based on the angle of attack.

$$C_D A = \frac{F_d \bullet v_1}{\frac{1}{2}\rho v^2} = L^2 \times \int \left\{ \begin{array}{l} 2(Sin(\chi)Cos(\alpha) + Cos(\chi)Cos(\zeta)Sin(\alpha))^2 \dfrac{Tan(\chi)}{Cos(\chi)} \\ \times (Sin(\chi)Cos(\alpha) + Cos(\chi)Cos(\zeta)Sin(\alpha)) \end{array} \right\} d\zeta$$

$$C_L A = \frac{F_d \bullet v_2}{\frac{1}{2}\rho v^2} = L^2 \times \int \left\{ \begin{array}{l} 2(Sin(\chi)Cos(\alpha) + Cos(\chi)Cos(\zeta)Sin(\alpha))^2 \dfrac{Tan(\chi)}{Cos(\chi)} \\ \times (Sin(\chi)Cos(\alpha) + Cos(\chi)Cos(\zeta)Cos(\alpha)) \end{array} \right\} d\zeta$$

where
$$\zeta_\pm = \left\{ \begin{array}{ll} \pm \pi & \text{when} \quad \alpha < \chi \\ \pm Cos^{-1}(-Tan(\chi)Ctn(\alpha)) & \text{when} \quad \alpha \geq \chi \end{array} \right\}$$

The graph of angle of attack vs C_D and C_L, resulting from these can be seen in the text in

Figure 2-2.

APPENDIX B: Equation of Variation

When we integrate the state vector through a given trajectory, we are concerned with more then just one ideal trajectory. We would like to be able to determine the characteristics of nearby trajectories. We define the phi matrix , Φ, as the n-dimensional matrix of small differences between some reference trajectory and a given trajectory very near it. The use of a phi matrix allows us to specify how initial errors in the trajectory propagate through to final errors. In order to obtain a final phi, we must have an equation of motion to propagate the phi matrix. In order to generate this equation, we will start with a reference or ideal trajectory and another trajectory which starts from a point whose initial conditions are the original I.C.'s plus a small δx as seen in Figure B-1.
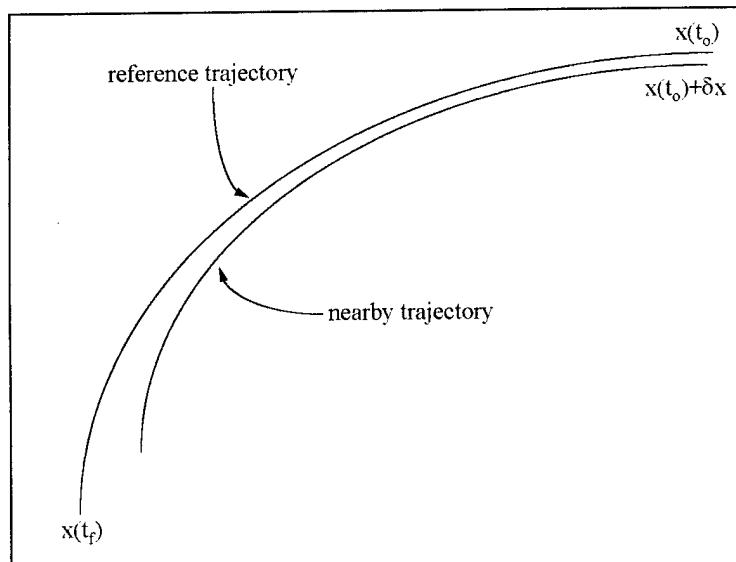
Figure B-1 Reference Trajectory

Now if we take the equation of the nearby trajectory to be $x = x_r(t) + \delta x(t)$, we

get the following equation of motion for the nearby trajectory,

$$\dot{x} = \dot{x}_r(t) + \delta\dot{x}(t) = f\big((x_r + \delta x), t\big).$$

Taking the Taylor series yields

$$\dot{x} \cong f(x_r, t) + \frac{\partial f}{\partial x}\bigg|_{x_r} \delta x + H.O.T..$$

We know that $\dot{x}_r(t) = f(x_r, t)$. Using this and truncating the higher order terms gives us the equation of variation as follows:

$$\delta\vec{\dot{x}} = \frac{\partial \vec{f}}{\partial \vec{x}} \delta\vec{x}$$

By the definition $A = \dfrac{\partial \vec{f}}{\partial \vec{x}}$ and this equation we get the equation of variation, $\delta\vec{\dot{x}} = A\delta\vec{x}$.

From the definition of the phi matrix, we know that it is simply the square matrix of the δx's. So we now have the following equation of variation:

$$\dot{\Phi} = A(t)\Phi$$

By convention, the phi matrix at time equals zero, $\Phi(t_0, t_0)$, is equal to the identity matrix, I. So we are now able to extend our knowledge of the reference trajectory to all the nearby trajectories by simply calculating the A matrix and using it in the equation of variation.

APPENDIX C: A Matrix Equations

$$\frac{\partial \dot{r}}{\partial r} = 0$$

$$\frac{\partial \dot{r}}{\partial \theta} = 0$$

$$\frac{\partial \dot{r}}{\partial \phi} = 0$$

$$\frac{\partial \dot{r}}{\partial v} = \text{Sin}\gamma$$

$$\frac{\partial \dot{r}}{\partial \gamma} = v\text{Cos}\gamma$$

$$\frac{\partial \dot{r}}{\partial \psi} = 0$$

$$\frac{\partial \dot{\theta}}{\partial r} = -\frac{v\text{Cos}\gamma\text{Cos}\psi\text{Sec}\theta}{r^2}$$

$$\frac{\partial \dot{\theta}}{\partial \theta} = 0$$

$$\frac{\partial \dot{\theta}}{\partial \phi} = \frac{v\text{Cos}\gamma\text{Cos}\psi\text{Sec}\phi\text{Tan}\phi}{r}$$

$$\frac{\partial \dot{\theta}}{\partial v} = \frac{\text{Cos}\gamma\text{Cos}\psi\text{Sec}\phi}{r}$$

$$\frac{\partial \dot{\theta}}{\partial \gamma} = \frac{-v\text{Cos}\psi\text{Sin}\gamma\text{Sec}\phi}{r}$$

$$\frac{\partial \dot{\theta}}{\partial \psi} = \frac{-v\text{Cos}\gamma\text{Sin}\psi\text{Sec}\phi}{r}$$

$$\frac{\partial \dot{\phi}}{\partial r} = -\frac{v\text{Cos}\gamma\text{Sin}\psi}{r^2}$$

$$\frac{\partial \dot{\phi}}{\partial \theta} = 0$$

$$\frac{\partial \dot{\phi}}{\partial \phi} = 0$$

$$\frac{\partial \dot{\phi}}{\partial v} = \frac{\text{Cos}\gamma\text{Sin}\psi}{r}$$

$$\frac{\partial \dot{\phi}}{\partial \gamma} = \frac{-v\text{Sin}\gamma\text{Sin}\psi}{r}$$

$$\frac{\partial \dot{\phi}}{\partial \psi} = \frac{v\text{Cos}\gamma\text{Cos}\psi}{r}$$

$$\frac{\partial \dot{v}}{\partial r} = 0$$

$$\frac{\partial \dot{v}}{\partial \theta} = 0$$

$$\frac{\partial \dot{v}}{\partial \phi} = 0$$

$$\frac{\partial \dot{v}}{\partial v} = -\frac{C_d\rho Sv}{m}$$

$$\frac{\partial \dot{v}}{\partial \gamma} = -g\text{Cos}\gamma$$

$$\frac{\partial \dot{v}}{\partial \psi} = 0$$

$$\frac{\partial \dot{\gamma}}{\partial r} = -\frac{v Cos\gamma}{r^2} - \frac{SC_L v^2 Cos\sigma}{2m}$$

$$\frac{\partial \dot{\gamma}}{\partial \theta} = 0$$

$$\frac{\partial \dot{\gamma}}{\partial \phi} = 0$$

$$\frac{\partial \dot{\gamma}}{\partial v} = \frac{\left(\dfrac{C_L \rho Sv Cos\sigma}{m} + \dfrac{2v Cos\gamma}{r}\right)}{v} - \frac{\left(\dfrac{C_L \rho Sv Cos\sigma}{2m} - \left[g - \dfrac{v^2}{r}\right]Cos\gamma\right)}{v^2}$$

$$\frac{\partial \dot{\gamma}}{\partial \gamma} = \left(g - \frac{v^2}{r}\right)Sin\gamma$$

$$\frac{\partial \dot{\gamma}}{\partial \psi} = 0$$

$$\frac{\partial \dot{\psi}}{\partial r} = \frac{v Cos\psi Cos\gamma Tan\phi}{r^2}$$

$$\frac{\partial \dot{\psi}}{\partial \theta} = 0$$

$$\frac{\partial \dot{\psi}}{\partial \phi} = -\frac{v Cos\psi Cos\gamma Sec^2\phi}{r}$$

$$\frac{\partial \dot{\psi}}{\partial v} = \frac{C_L \rho S Sec\gamma Sin\sigma}{2m} - \frac{Cos\psi Cos\gamma Tan\phi}{r}$$

$$\frac{\partial \dot{\psi}}{\partial \gamma} = \frac{v Cos\psi Sin\gamma Tan\phi}{r} + \frac{v C_L \rho S Tan\gamma Sec\gamma Sin\sigma}{2m}$$

$$\frac{\partial \dot{\psi}}{\partial \psi} = \frac{v Cos\gamma Sin\psi Tan\phi}{r}$$

Appendix D: B Matrix Equations

$$\frac{\partial \dot{r}}{\partial \sigma} = 0$$

$$\frac{\partial \dot{\theta}}{\partial \sigma} = 0$$

$$\frac{\partial \dot{\phi}}{\partial \sigma} = 0$$

$$\frac{\partial \dot{v}}{\partial \sigma} = \frac{\rho v^2}{2m} \frac{\partial (SC_D)}{\partial \sigma} = 0$$

$$\frac{\partial \dot{\gamma}}{\partial \sigma} = \frac{\rho v}{2m} \frac{\partial (SC_L)}{\partial \sigma} Cos\sigma - \frac{\rho SC_L v}{2m} Sin\sigma$$

$$\frac{\partial \dot{\psi}}{\partial \sigma} = \frac{\rho v}{2mCos\gamma} \frac{\partial (C_L)}{\partial \sigma} Sin\sigma + \frac{\rho SC_{Lv}}{2mCos\gamma} Cos\sigma$$

$$\frac{\partial \dot{r}}{\partial \varepsilon} = 0$$

$$\frac{\partial \dot{\theta}}{\partial \varepsilon} = 0$$

$$\frac{\partial \dot{\phi}}{\partial \varepsilon} = 0$$

$$\frac{\partial \dot{v}}{\partial \varepsilon} = \frac{\rho v^2}{2m} \frac{\partial (SC_D)}{\partial \varepsilon}$$

$$\frac{\partial \dot{\gamma}}{\partial \varepsilon} = \frac{\rho v}{2m} \frac{\partial (SC_L)}{\partial \varepsilon} Cos\sigma$$

$$\frac{\partial \dot{\psi}}{\partial \varepsilon} = \frac{\rho v}{2mCos\gamma} \frac{\partial (SC_L)}{\partial \varepsilon}$$

APPENDIX E: Flowchart for Program DESIGN
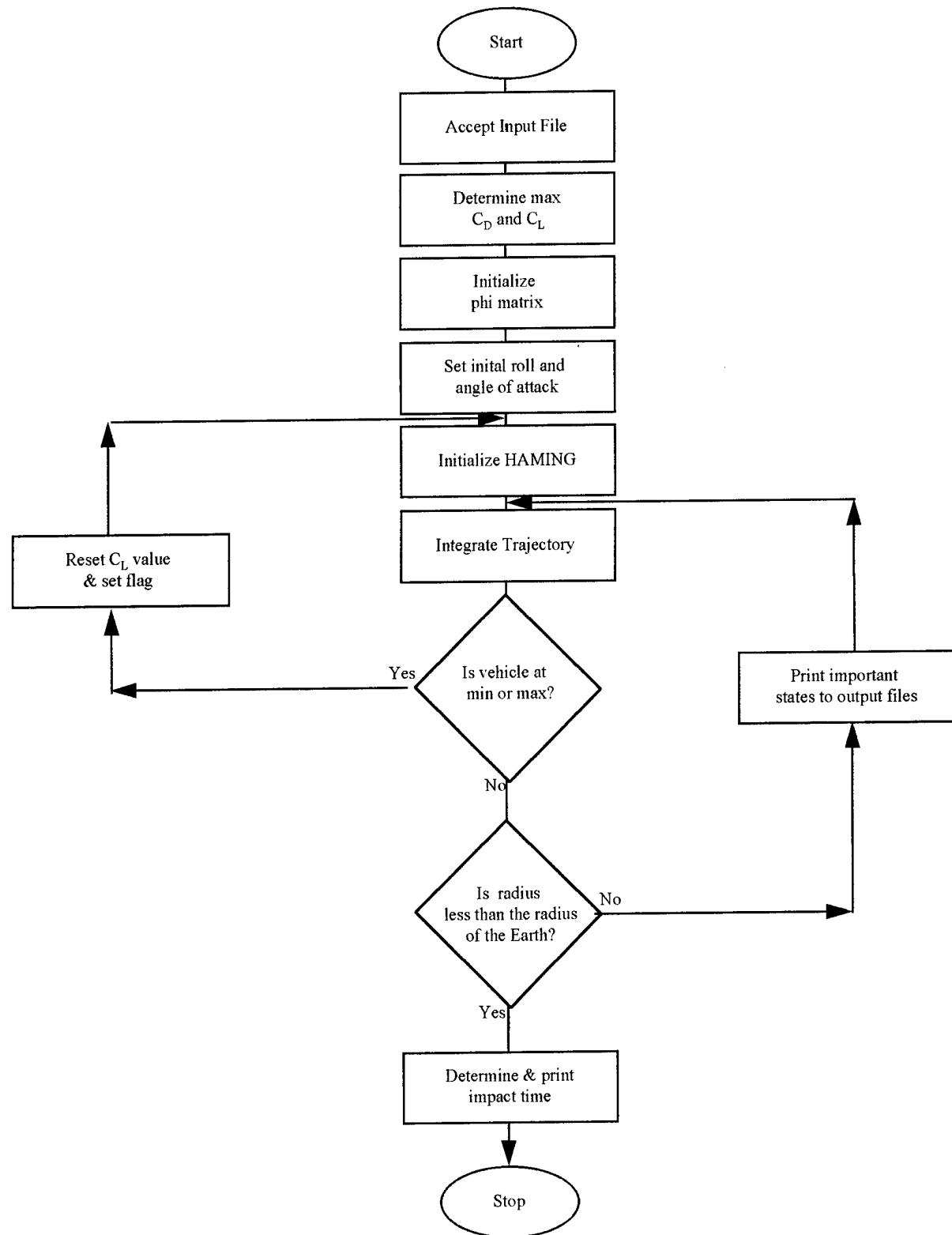
APPENDIX F: Flowchart for Program FIRST

```
                    ( Start )
                        |
            +-----------------------+
            |   Accept Input File   |
            +-----------------------+
                        |
            +-----------------------+
            |      Initialize       |
            |      phi matrix       |
            +-----------------------+
                        |
            +-----------------------+
            |   Initialize HAMING   |
            +-----------------------+
                        |
            +-----------------------+  <--------------------+
            |  Integrate Trajectory |                       |
            +-----------------------+                       |
                        |                                   |
            +-----------------------+                       |
            | Set angle of attack,roll,                     |
            |   C_D & C_L values                            |
            |   from  DESIGN        |                       |
            +-----------------------+                       |
                        |                                   |
                    / Is  radius \          No              |
                   < less than the radius >-----------------+
                    \ of the Earth? /
                        |
                      Yes
                        |
            +-----------------------+
            |   Determine & print   |
            |      impact time      |
            +-----------------------+
                        |
            +-----------------------+
            |     Determine phi     |
            +-----------------------+
                        |
            +-----------------------+
            |  Decompose phi matrix |
            +-----------------------+
                        |
            +-----------------------+
            | Calculate open loop Lyapunov
            |  exponents and principal
            |      directions       |
            +-----------------------+
                        |
            +-----------------------+
            |   Output two copies of
            | Lyapunov exponents and
            | principal directions to file
            +-----------------------+
                        |
                    ( Stop )
```

APPENDIX G: Flowchart for Program BVP

```
( Start )
   |
[ Accept Input File ]
   |
[ Construct Desired
  phi matrix ]
   |
[ Initialize phi & phi
  Lagangian matrix ]
   |
[ Initialize HAMING ]
   |
[ Integrate Trajectory ]<------------+
   |                                  |
  < Is radius                         |
    less than the radius >--No------->+
    of the Earth?
   |
  Yes
   |
[ Construct & print
  error vector ]
   |
[ Set delta value ]
   |
[ Set up Loop 1:
  1 to order ]
   |
[ Set up Loop 2:
  1 to order ]
   |
[ Initialize states, phi,
  & phi Lagrangian ]
   |
[ Perturb Loop1,Loop2
  element of phi
  Lagrangianby delta ]
   |
[ Initialize HAMING ]
   |
[ Integrate Trajectory ]<----(2)
   |
  (1)
```

```
  (1)
   |
  < Is radius
    less than the radius >--No---->(2)
    of the Earth?
   |
  Yes
   |
[ Determine phi
  perturbed ]
   |
[ Calculate phi
  Lagrangian partials ]
   |
[ Get phi
  Lagrangian at t=t0 ]
   |
[ Calculate S0 matrix ]
   |
[ Initialize states, phi,
  & phi Lagrangian ]
   |
[ Initialize HAMING ]
   |
[ Integrate Trajectory ]<------------+
   |                                  |
[ Print Gain matrix,                  |
  time and state ]                    |
   |                                  |
  < Is radius                         |
    less than the radius >--No------->+
    of the Earth?
   |
  Yes
   |
[ Determine & print
  final phi ]
   |
[ Calculate Lyapunov
  exponents and
  principal directions ]
   |
 ( End )
```

73

AERO

TYPE: Subroutine

PURPOSE: This routine iterates through a list of data points to determine the CD and CL values for a given angle of attack. Once the closest data point is found, the code uses interpolation to get the exact values of C_D and C_L. The numerical derivatives of C_D and C_L with respect to angle of attack are also calculated.

INPUTS: Angle of Attack

OUTPUTS: Coefficients of Drag and Lift
             Partials of the coefficients of Drag and Lift with respect to Angle of Attack

CALLS: None

AUTHOR: William E. Wiesel

ATM

TYPE: Subroutine

PURPOSE: This routine determines the temperature, density and pressure at the current altitude of the vehicle.

INPUTS: Altitude, Density at sea level

OUTPUTS: Pressure, Temperature, and Density at altitude.

CALLS: None

AUTHOR: Michael H. Platt

BVP

TYPE: Main Program

PURPOSE: This program solves the boundary value problem such that the
                numerical partials of the phi matrix are determined and used to determine
                what gain will be needed to achieve the final Lyapunov exponents and
                principal direction vectors.

INPUTS: State initial Conditions
                Control history of flight
                Open loop Lyapunov exponents and principal direction vectors, U and V
                Desired closed loop Lyapunov exponents and principal vectors U and V

OUTPUTS: Gain as a function of time
                Achieved phi matrix
                Achieved Lyapunov exponents and principal direction vectors, U and V

CALLS: HAMING
                LEQT2F
                LINV1F
                SVDCMP

AUTHOR: Dr William E. Wiesel
                        modified by Michael H. Platt

DESIGN

TYPE: Main Program

PURPOSE: The purpose of this program is to design the reentry trajectory of the
                vehicle based on the initial conditions provided. This code makes use of a
                control law which is specified in the text of this paper.

INPUTS: Initial state conditions
                Parameter values
                initial control variables

OUTPUTS: Control history of trajectory
                Miscellaneous plot files
                Final state and control values

CALLS: AERO
                HAMING

AUTHOR: Dr William E. Wiesel
                        modified by Michael H. Platt

DYNAM

TYPE: Subroutine

PURPOSE: This subroutine implements the control law which keeps the vehicle at maximum altitude for as long as possible. It also calls the various subroutines to determine CD, CL, and characteristics of the atmosphere at altitude.

INPUTS: nxt (flag)

OUTPUTS: Equations of Motion
A matrix
B matrix

CALLS: AERO
ATM

AUTHOR: Dr William E. Wiesel
             modified by Michael H. Platt

FIRST

TYPE: Main Program

PURPOSE: This program iterates through the trajectory, takes the phi matrix, decomposes it and calculates the open loop Lyapunov exponents and the principal direction vectors, U and V. It then outputs these to a file which will eventually be used in the program BVP.

INPUTS: Initial Conditions
Parameters
Control History of Trajectory

OUTPUTS: Open Loop Lyapunov exponents
Open Loop Principal Direction Vectors

CALLS: HAMING
SVDCMP

AUTHOR: Dr William E. Wiesel
             modified by Michael H. Platt

HAMING

TYPE: Subroutine

PURPOSE: This routine is an ordinary differential equations integrator. It uses a
            fourth order predictor-corrector algorithm such that it carries along the last
            four values of the state vector. It extrapolates these values to obtain the
            next value (the prediction part) and then corrects the extrapolated value to
            find a new value for the state vector.

INPUTS: state vector

OUTPUTS: State vector

CALLS: RHS

AUTHOR: Dr William E. Wiesel

LEQTF

TYPE: Subroutine

PURPOSE: This routine is a linear equation solver, which makes use of Gaussian
            elimination with maximal pivoting.

INPUTS: Matrices A and B from the equation Ax=B

OUTPUTS: x from the above equation

CALLS: None

AUTHOR: IMSL

LINV1F

TYPE: Subroutine

PURPOSE: This subroutine inverts a matrix.

INPUTS: Matrix to be inverted

OUTPUTS: Inverted matrix

CALLS: None

AUTHOR: IMSL

RHS

TYPE: Subroutine

PURPOSE: This routine calculates the quantity A phi which can be used to update the phi matrix.

INPUTS: state vector

OUTPUTS: Equations of Motion
A phi

CALLS: DYNAM

AUTHOR: Dr William E. Wiesel
modified by Michael H. Platt

SVDCMP

TYPE: Subroutine

PURPOSE: This routine performs the singular value decomposition of the input matrix.

INPUTS: Matrix top be decomposed

OUTPUTS: Resulting vectors and diagonal matrix

CALLS: None

AUTHOR: "Numerical Recipes" [pp60-64]

APPENDIX I: Input Files

DESIGN.IN

\# of States, \# of Parameters, \# of Controls
Parameters
Initial State Conditions (radius, longitude, latitude, velocity, flight path angle, heading)
Initial Control Conditions (roll, pitch)
Maximum Time, \# of Points, \# of Points to Skip

FIRST.IN

\# of States, \# of Parameters, \# of Controls
Parameters
Initial State Conditions (radius, longitude, latitude, velocity, flight path angle, heading)
Initial Control Conditions (roll, pitch)
Maximum Time, \# of Points, \# of Points to Skip

BVP.IN

\# of States, \# of Parameters, \# of Controls
Parameters
Initial State Conditions (radius, longitude, latitude, velocity, flight path angle, heading)
Initial Control Conditions (roll, pitch)
Maximum Time, \# of Points, \# of Points to Skip
Open Loop Lyapunov Exponents
Open Loop Principal Direction Vectors U and V
Desired Closed Loop Lyapunov Exponents
Desired Closed Loop Principal Direction Vectors U and V
Order of Control Matrix
Control Matrix

APPENDIX J: Open Loop Dynamical Direction Vectors

<u>CASE 1</u>

		<u>u</u>	<u>v</u>
1	1	-0.01028543050235800060	-0.97168401832455997269
2	1	0.00363444199734480004	0.00003107162937948000
3	1	-0.0000000000000469740	0.00000000000002290337
4	1	0.08214474583247899364	-0.03569012010809000102
5	1	0.99656070637109994692	-0.23357307827285000990
6	1	-0.00000000001125988246	-0.00000000000009349885

1	2	-0.00089665641974298995	0.00796246377915789914
2	2	-0.99996954401282001079	-0.97579409007383999253
3	2	-0.00000000000011928163	0.00000000000453068203
4	2	0.00712768995717460042	-0.21854627299113998928
5	2	0.00305009670780599998	0.00013967542602473000
6	2	-0.00000000001996683656	-0.00000000001895038530

1	3	-0.12171244904868999681	0.22179652742774000340
2	3	0.00690662913636379966	0.10524131864098999756
3	3	0.00000000000000457848	-0.00000000000204756123
4	3	0.98908086295801000976	-0.46235891461048000961
5	3	-0.08280956919816499784	-0.85202981130470001325
6	3	0.00000000000058194711	0.00000000000862846213

1	4	-0.99251170555979995047	-0.08107446036942800305
2	4	0.00001876508221094700	0.19170330634143001314
3	4	-0.00000000000000005374	0.00000000000001332149
4	4	-0.12214943020019999875	-0.85859651523201996337
5	4	-0.00017514685499890999	0.46849631614879999608
6	4	-0.00000000000000003907	-0.00000000000008494051

1	5	-0.00000000000006291855	-0.0000000000191225029
2	5	-0.0000000001992965083	-0.0000000001992963855
3	5	0.00771671613673619982	-0.23082828392586998700
4	5	0.00000000000049162056	-0.00000000000023507429
5	5	0.00000000001132995245	0.00000000000757627134
6	5	0.99997022570278004672	0.97299450324236003151

1	6	0.00000000000000096663	0.0000000000000000000
2	6	0.00000000000003463015	0.00000000000003458703
3	6	0.99997022570278004672	0.97299450324236003151
4	6	-0.00000000000000700461	0.00000000000000149329
5	6	-0.00000000000008201465	0.00000000000000278481
6	6	-0.00771671613673600033	0.23082828392586998700

CASE 2 (0.0 - 1.0 TU)

		u	v
1	1	-0.06513334848611600225	-0.98233526721117003788
2	1	0.08123799463349500039	0.00001966208784733900
3	1	-0.09214490890452099736	0.00012344799140762001
4	1	0.40856082818428002268	-0.03676190204151300045
5	1	-0.53349110099935004303	-0.18348284244442000790
6	1	-0.72741504365373998997	-0.00012749098910065000
1	2	-0.05909772630751399664	0.10507018593484999947
2	2	-0.42440813732748000620	-0.08834185895499800656
3	2	0.34883167171661999539	-0.00026492752091081002
4	2	-0.29514532828202000303	-0.90984883644657998936
5	2	-0.72701775086806996740	-0.38030822618972998095
6	2	0.28113356547897999649	0.09325582934395500179
1	3	-0.99488239960038005183	-0.12758862379124999431
2	3	0.00000217186183196260	0.03746385565551300229
3	3	0.00002335921155600400	-0.10489380108456000662
4	3	-0.03458991987095100251	-0.26425770193451997292
5	3	0.09493443608945199841	0.73554924314832004217
6	3	0.00002650879976210500	0.60037494198603003071
1	4	0.00659393826681990008	-0.06457644432611399365
2	4	-0.61186947499749000379	-0.56030766996837999550
3	4	-0.77535346913045000150	-0.39874751101654998253
4	4	-0.14171256413912999839	-0.17243074346014000686
5	4	0.01769099672166399989	0.38036046915558002768
6	4	-0.06327591367903200037	-0.59032124515761996708
1	5	-0.02818112547849700028	0.05840774375848799965
2	5	-0.29353527557349001764	-0.49957398211156001100
3	5	0.04090872648305499820	-0.53008406985981004755
4	5	0.85124937207759998614	0.26096667465457001889
5	5	0.01470462107028499936	-0.36575846116713001122
6	5	0.43188843804269999582	0.51394785100386997101
1	6	0.04045319234070700321	-0.01082775170848999935
2	6	-0.59391153276705999087	-0.65366147695959997410
3	6	0.51670035226388999483	0.74095108233067996650
4	6	-0.00792956572542049924	0.05617435155750000186
5	6	0.42105901091864000874	0.04704967707934799848
6	6	-0.44866447124517999656	0.13502480156904000941

CASE 3 (0.0 - 1.0 TU)

		u	**v**
1	1	-0.06389959006247300510	-0.98258845740532996249
2	1	0.07831410885031099556	0.00001413839874403200
3	1	-0.07481340127633999415	0.00009350141821937500
4	1	0.36301192648443997291	-0.03477221682566800087
5	1	-0.56829488266759997650	-0.18251246080158001206
6	1	-0.72763312548164005289	-0.00009497680907610600
1	2	-0.05264048512495699689	0.10385091218924000223
2	2	-0.46576529173300001974	-0.10843137532169999648
3	2	0.31555588699281000853	-0.01516064742741900055
4	2	-0.30706995163021000295	-0.90317797911088004703
5	2	-0.69832947170930004255	-0.38709910220319998508
6	2	0.31426127390260000238	0.10794259018358999536
1	3	0.00508511554381889993	-0.06392369442280200487
2	3	-0.52968321718317001867	-0.48472424352228998812
3	3	-0.83826363559234995382	-0.48575829257165997754
4	3	-0.12253006393467000268	-0.17365098034786000114
5	3	0.00992349524661539917	0.37725113305793001039
6	3	-0.04014742771513900299	-0.59373560602483999027
1	4	0.99534969609505996591	0.12658611719581999711
2	4	-0.00000171062338637060	-0.03617232547061600273
3	4	-0.00001901692147163200	0.10619068515049999435
4	4	0.03415835918811700039	0.25712774058570997404
5	4	-0.09006768631214200072	-0.73011780701259998416
6	4	-0.00002233515044160400	-0.61008554244057000560
1	5	-0.03071106195926399940	0.05812527505084000290
2	5	-0.26391747948327998197	-0.45890691292737001428
3	5	0.01941350196523499924	-0.55742526528196001401
4	5	0.87042914625278000607	0.28956397897627000892
5	5	-0.00938157158515089996	-0.36867962124332998020
6	5	0.41387509964507002147	0.50550075198002997201
1	6	0.03815463893647400018	-0.01568693839398100157
2	6	-0.65323261310700997395	-0.73578601000916998842
3	6	0.43790938560041997585	0.66468762530795999499
4	6	0.01015270009756000062	0.05425675175635699676
5	6	0.42553283952603998541	0.07435317138578399765
6	6	-0.44596577432547002129	0.08995020286136899690

CASE 4 (0.0 -0.25 TU)

		u	v
1	1	-0.00424501835640509959	-0.98275212517203003326
2	1	0.00486853551608860003	0.00002020102189509900
3	1	0.00051177705371614995	0.00014408704217409000
4	1	-0.00365524018172130004	-0.01788005846675300159
5	1	-0.98150231201513005175	-0.18405959217574999198
6	1	-0.19130568730045999226	-0.00078060107066167997
1	2	0.00015856428007883001	0.02342717615886300009
2	2	-0.98598227258126003303	-0.96373444626989002160
3	2	-0.03237860992992400155	-0.00289809927635030018
4	2	0.00068161489029038003	-0.18260604405283001328
5	2	0.02656846007968500026	-0.10677154859475999904
6	2	-0.16150607097566999082	-0.16097687596897999884
1	3	0.00081477086986990997	0.01779211106295799927
2	3	0.16243344365060999324	0.16460224394226000144
3	3	0.03600438154295500237	0.21131587728035000628
4	3	0.00096219023103698005	0.02973016257455799935
5	3	0.18943181631452998825	-0.09363821513029199628
6	3	-0.96769471332630996319	-0.95827091377273998507
1	4	0.00002274309356453900	0.00168081358645540005
2	4	0.03781992876969399869	0.03781834147168299659
3	4	-0.99882683543490002887	-0.97735343387202000542
4	4	0.00004280878599849200	0.00489308065307680028
5	4	0.00546410109994549965	-0.00932881973904150022
6	4	-0.02974469788537199844	-0.20793326837375000760
1	5	-0.03369417688200600225	-0.17241850223978999468
2	5	-0.00053312347196117005	-0.15944814598802001249
3	5	-0.00003206112777283000	0.00892191453331350054
4	5	-0.99942425398929002345	0.39359067675171000023
5	5	0.00393192329604650018	0.88278711677471999320
6	5	-0.00034309305819740999	-0.10267343326363999323
1	6	-0.99942282981326002744	0.06001586142085699876
2	6	-0.00002585417719523500	-0.13140806574665001016
3	6	0.00000039281516633206	-0.00615182967721980035
4	6	0.03371064395236499783	0.90028544948462996267
5	6	0.00419511431231320026	-0.40810987146214000587
6	6	0.00000892650091013410	0.04499570965845500065

CASE 5

		u	**v**
1	1	-0.01041367828494699915	-0.97167057239938003921
2	1	0.00337819864074320004	0.00002933637589193600
3	1	0.00000000000001214309	0.00000000000001827429
4	1	0.08037935879455899990	-0.03571246813911099771
5	1	0.99670421979557000114	-0.23362559254466999659
6	1	-0.00000000000877931300	-0.00000000000007401808

1	2	-0.00088850219598885004	0.00792159671889250058
2	2	-0.99997201756267994899	-0.97580439758499004643
3	2	-0.00000000000015860298	0.00000000000341644084
4	2	0.00686937597676139967	-0.21850152435160000164
5	2	0.00282600940400740000	0.00033138383146531000
6	2	-0.00000000001535902870	-0.00000000001457042648

1	3	-0.12504998895203001119	0.22178708445351999479
2	3	0.00667469197903149992	0.10521059958065999418
3	3	0.00000000000000257644	-0.00000000000127910980
4	3	0.98881004102974001668	-0.46311014966396002457
5	3	-0.08107189099091000051	-0.85162797522375000003
6	3	0.00000000000035182400	0.00000000000539344279

1	4	-0.99209539164917004417	-0.08126522139322900351
2	4	0.00001877611933808500	0.19166769818894999200
3	4	0.00000000000000014074	-0.00000000000016630747
4	4	-0.12548574864192998946	-0.85820201162293996422
5	4	-0.00024577166175789001	0.46920013268241000937
6	4	0.00000000000000001726	0.00000000000074047692

1	5	-0.00000000000006105413	-0.00000000000112323390
2	5	-0.00000000001533198355	-0.00000000001533197506
3	5	0.00627845312630180043	-0.23224721542661000417
4	5	0.00000000000046327297	-0.00000000000005440161
5	5	0.00000000000882206040	0.00000000000435169797
6	5	0.99998029031892998741	0.97265678989383996811

1	6	0.00000000000000088139	0.00000000000000000000
2	6	-0.00000000000006234910	-0.00000000000006240077
3	6	0.99998029031892998741	0.97265678989383996811
4	6	-0.00000000000000529162	-0.00000000000000078611
5	6	-0.00000000000006683849	0.00000000000000261258
6	6	-0.00627845312630120021	0.23224721542661000417

APPENDIX K: Closed Loop Dynamical Direction Vectors

Case1 (Full Trajectory)

		u	**v**
1	1	-0.01030196743589699947	-0.97168348266467996499
2	1	0.00363519794936909999	0.00003598647879645000
3	1	-0.00000269712930276840	0.00000695859965293510
4	1	0.08215147129278900506	-0.03570886302410700153
5	1	0.99655997723858003035	-0.23357243750167999696
6	1	-0.00004823075400571100	-0.00004140344651853700
1	2	-0.00089705510246072004	0.00796202149669830023
2	2	-0.99996953333970994837	-0.97579391837360995865
3	2	-0.00000007726882264421	0.00000132604342975910
4	2	0.00712887931237249969	-0.21854705630080001333
5	2	0.00305069197477219993	0.00013865925542491000
6	2	-0.00000653618027104730	-0.00000573366677570370
1	3	-0.12170074252679000115	0.22180600744673001357
2	3	0.00690777256897090030	0.10524011426266000058
3	3	0.00000126580746497530	-0.00000708564145476850
4	3	0.98908156631773003209	-0.46234794239902998747
5	3	-0.08281826900950700621	-0.85203344554194004878
6	3	0.00003786428065245200	0.00003460671460691000
1	4	0.99251295011246998268	0.08105497925627799805
2	4	-0.00001903828123642700	-0.19170483534745000331
3	4	-0.00000134867301182800	0.00004290624056404200
4	4	0.12213914161319999740	0.85860142768133995705
5	4	0.00019164511472974000	-0.46849002173213999400
6	4	-0.00019197112673628001	-0.00018033916462201999
1	5	0.00019464471915760001	-0.00003346437354563100
2	5	-0.00000662625511493670	-0.00004499363566479400
3	5	0.00766005984867070000	-0.23088536749260998859
4	5	-0.00001000118430728300	0.00017270391510402000
5	5	0.00005127731661911400	-0.00006654596705623000
6	5	0.99997064098065002735	0.97298094003864998847
1	6	-0.00000002622088171184	-0.00000296158151728740
2	6	-0.00000002547469277593	-0.00000012708358433498
3	6	0.99997066130583001087	0.97298095825996000485
4	6	-0.00000078855055026103	0.00000030596932204931
5	6	0.00000240046040188910	0.00000033361930094311
6	6	-0.00766006013041200043	0.23088537167723999222

Case 2 (0.0-1.0 TU)

		$\underline{u}$	$\underline{v}$
1	1	-0.06403794634675200048	-0.98197198903211002641
2	1	0.08104454666619399783	0.00003854206213596400
3	1	-0.09152908323148399583	0.00034680135676126998
4	1	0.40839753831084002478	-0.03735085165286099879
5	1	-0.53423972957695997632	-0.18529866553367999038
6	1	-0.72715384331608001744	-0.00045763730138782002
1	2	-0.05903755451191700088	0.10628079270262999478
2	2	-0.42448063072810998664	-0.08834193353221600487
3	2	0.34891450328283002413	-0.00026562707974199003
4	2	-0.29551058145622000062	-0.90980191219835004901
5	2	-0.72653876711373999164	-0.38008400816391002541
6	2	0.28178776911191000254	0.09325584497946799722
1	3	-0.99495714713326000034	-0.12900962363557000323
2	3	0.00009601858723680201	0.03746454580284599989
3	3	-0.00008003936800790900	-0.10489259283410999612
4	3	-0.03411823921992700182	-0.26431336390713000561
5	3	0.09431619478986699723	0.73528040842211994654
6	3	-0.00081295477612005002	0.60037624489685004203
1	4	-0.00656852952997049981	0.06508464381380499320
2	4	0.61184116433513002775	0.56030832780411998773
3	4	0.77538594511035996426	0.39874807164386000258
4	4	0.14156557938782998729	0.17245108740557998916
5	4	-0.01749934702153600058	-0.38026589288300999270
6	4	0.06353612953725400192	0.59031941815917998717
1	5	0.02817996314232600052	-0.05863769153244700189
2	5	0.29353482224404997547	0.49957296615830998343
3	5	-0.04090995975545200225	0.53008397131011997239
4	5	-0.85124432762849999712	-0.26097697232051997318
5	5	-0.01471300783230499939	0.36571538624006999507
6	5	-0.43189836198010000956	-0.51394818042416001713
1	6	0.04045649577632599858	-0.01084127020287400066
2	6	-0.59391553619007997344	-0.65366163906047003440
3	6	0.51670504277926998515	0.74095095104871999681
4	6	-0.00794821454630850049	0.05617368131237700235
5	6	0.42108323034417999287	0.04704656477642599893
6	6	-0.44863041091354000089	0.13502501579976000645

Case 3 (0.0-1.0 TU)

		u	**v**
1	1	-0.06278771840705099638	-0.98192814311970999519
2	1	0.07758655902839599328	0.00009643533037484300
3	1	-0.07308126470797199348	0.00049327354493162003
4	1	0.36251257820206000959	-0.03680018579577300220
5	1	-0.57034039074792997059	-0.18564101112188000076
6	1	-0.72663169924717996295	0.00017448767022450000
1	2	-0.05246989309574699722	0.10692042755274999699
2	2	-0.46597925612702001397	-0.10843304324871999578
3	2	0.31575448226028002274	-0.01516354659180800014
4	2	-0.30805768113385001428	-0.90306699128979994740
5	2	-0.69677893169020999053	-0.38652152013084001281
6	2	0.31624189405809999265	0.10794205796189999813
1	3	0.00502321536616699964	-0.06516520699071000344
2	3	-0.52959933437120998434	-0.48472447768119997225
3	3	-0.83834300983364995474	-0.48575794479201001019
4	3	-0.12214355309983999931	-0.17369187049047998816
5	3	0.00932162215460139928	0.37701522525385999796
6	3	-0.04091906646739700004	-0.59373862065583005165
1	4	0.99543029559637996595	0.12827746061542000255
2	4	-0.00009858415344814100	-0.03616913545493599669
3	4	0.00007994123973226300	0.10619360079761999693
4	4	0.03369496482236500334	0.25718811750865999688
5	4	-0.08934395475991299684	-0.72980305301406001028
6	4	0.00090420846448446000	-0.61008309426818996268
1	5	0.03069744553109399893	-0.05859718947410400003
2	5	0.26393126842742997695	0.45890617494841001722
3	5	-0.01942787267304599969	0.55742494271582998522
4	5	-0.87036042917246003725	-0.28958219051766997953
5	5	0.00927288390453519934	0.36859270286652001669
6	5	-0.41401358323414000351	-0.50550024683154004546
1	6	-0.03815197884664100342	0.01580829538758799988
2	6	0.65322927030137001303	0.73578622085724998403
3	6	-0.43790613710825998517	-0.66468744158085002471
4	6	-0.01016960432960200070	-0.05425234410640199928
5	6	-0.42550644856043001729	-0.07433015940442400105
6	6	0.44599888272934001821	-0.08995026714864599870

Case 4 (0.0-0.2 TU)

		u	**v**
1	1	0.00407560477945550018	0.98291684951499003198
2	1	-0.00487234534914969975	0.00006991163479859799
3	1	-0.00051323591184877998	-0.00019469659306152999
4	1	0.00447495449078090003	0.01772321612742299921
5	1	0.98145270338973999991	0.18319148775701998844
6	1	0.19154621394497001186	0.00109113179880259998
1	2	-0.00016394463631259001	-0.02343298383793299827
2	2	0.98598421230249999603	0.96373990106692997148
3	2	0.03237821518398800030	0.00289931053690890015
4	2	-0.00065507830183980003	0.18260103730450000237
5	2	-0.02660171169414399933	0.10674047139919000393
6	2	0.16148893832468000364	0.16096964092386001344
1	3	0.00081850249847946000	0.01800059560175500117
2	3	0.16242177366460000543	0.16459064390700001157
3	3	0.03600486866152999982	0.21131676834402998710
4	3	0.00095321871769173995	0.02973311783532000055
5	3	0.18966981630667001379	-0.09358959244208800432
6	3	-0.96765003957124995360	-0.95827347443369004232
1	4	0.00002362447437384800	0.00168374693179929990
2	4	0.03781926605567499655	0.03781689603535000332
3	4	-0.99882683009985995248	-0.97735319227367001282
4	4	0.00003680641205110400	0.00489445487060819959
5	4	0.00547029621903729994	-0.00932235185911369987
6	4	-0.02974458831665499972	-0.20793490084717999866
1	5	0.03369177436230599842	0.17153162469818999947
2	5	0.00051280696685644005	0.15942269880883000455
3	5	0.00002598670125070800	-0.00892565734256530081
4	5	0.99942094042370999141	-0.39361250849436002497
5	5	-0.00472805468852129963	-0.88295663680890001945
6	5	0.00017330743813465999	0.10265674914884000135
1	6	-0.99942361209034003000	0.05979471122629299862
2	6	-0.00003040863980805300	-0.13141386388390999262
3	6	-0.00000065150278624133	-0.00615221112746930018
4	6	0.03371082195183500163	0.90027991644683003081
5	6	0.00400275957858800026	-0.40815316982269000956
6	6	-0.00003271507700252800	0.04499112349002200306

Case 5 (Full Trajectory)

		u	**v**
1	1	-0.01041530053179800033	-0.97167013709261995658
2	1	0.00337808160847269997	0.00002980091470781400
3	1	-0.00000047045397049255	0.00000118715607556220
4	1	0.08038163439867100635	-0.03571525579333000022
5	1	0.99670401965090005270	-0.23362697668509999072
6	1	-0.00011193261960161800	-0.00000784210261012930
1	2	-0.00088854274873018005	0.00792175728112910066
2	2	-0.99997201770775001606	-0.97580438366291000207
3	2	-0.00000000807164993311	-0.00000004128749735507
4	2	0.00686940589491800025	-0.21850158067385000438
5	2	0.00282587259153440013	0.00033140435482745002
6	2	0.00000016311292912141	0.00000011574655821605
1	3	0.12504809255749999020	-0.22178979420664998723
2	3	-0.00667472935027269964	-0.10521024529781000667
3	3	-0.00000042080464192042	0.00000103491962083450
4	3	-0.98881007888376004633	0.46310826072090999217
5	3	0.08107435086673600577	0.85162834046241997488
6	3	-0.00000806762111479700	-0.00000650769066518860
1	4	0.99209561234791998618	0.08126301495186599722
2	4	-0.00001882075046282100	-0.19166796324950999275
3	4	-0.00000025218505800159	0.00001048813803644300
4	4	0.12548399105543001086	0.85820289960444995359
5	4	0.00024724356235660000	-0.46919878021680000435
6	4	-0.00004965017436717500	-0.00004368402372055200
1	5	0.00005014330648767700	-0.00000548684001444840
2	5	0.00000014857307140196	-0.00000918255128935160
3	5	0.00625139842847079966	-0.23227629793377999046
4	5	-0.00000079115124702147	0.00004134220013669600
5	5	0.00001256208153426500	-0.00001733014940955000
6	5	0.99998045848150995951	0.97264984413417998610
1	6	-0.00000001556067545741	-0.00000076427793797184
2	6	-0.00000001022468468011	-0.00000005560964818876
3	6	0.99998045981770000701	0.97264984516818997484
4	6	-0.00000034164025119689	0.00000016034660024542
5	6	0.00000042458270688477	0.00000029983772252792
6	6	-0.00625139844164640003	0.23227629817439998661

Vita

Captain Mike Platt was born on 10 February 1967, in Wanaque, New Jersey. He graduated from Lakeland Regional High School in Wanaque and attended the U.S. Air Force Academy, graduating with a Bachelor of Science in Astronautical Engineering in May 1989. Upon graduation, he served his first tour of duty at Los Angeles AFB, California. His jobs during this time included financial officer for the Inertial Upper Stage Program Office, System Threat Engineer for the Directorate of Intelligence and a special year long tour as an analyst for the Aerospace Corporation, El Segundo, CA. He entered the School of Engineering, Air Force Institute of Technology, in June of 1994. His next assignment is at Phillips Laboratory, Kirtland AFB, New Mexico.

Permanent Address:

576 Ringwood Ave
Wanaque, N.J. 07465

REPORT DOCUMENTATION PAGE

Form Approved
OMB No. 0704-0188

1. AGENCY USE ONLY (Leave blank)	2. REPORT DATE December 1995	3. REPORT TYPE AND DATES COVERED Master's Thesis

4. TITLE AND SUBTITLE

Full Lyapunov Exponent Placement In Reentry Trajectories

5. FUNDING NUMBERS

6. AUTHOR(S)

Michael H. Platt, Captain, USAF

7. PERFORMING ORGANIZATION NAME(S) AND ADDRESS(ES)

Air Force Institute of Technology
2750 P Street
WPAFB, OH 45433-6583

8. PERFORMING ORGANIZATION REPORT NUMBER

AFIT/GA/ENY/95D-03

9. SPONSORING/MONITORING AGENCY NAME(S) AND ADDRESS(ES)

Lt Col J. Sponable
Phillips Lab/VT-X
3515 Aberdeen Ave.
Kirtland AFB, NM 87117

10. SPONSORING/MONITORING AGENCY REPORT NUMBER

11. SUPPLEMENTARY NOTES

12a. DISTRIBUTION/AVAILABILITY STATEMENT

Approved for public release; distribution unlimited

12b. DISTRIBUTION CODE

13. ABSTRACT (Maximum 200 words)

This study investigated the ability to control the chaotic reentry of a Delta-Clipper like vehicle by setting the values of initial and final principal dynamical directions as well as the Lyapunov exponents. A model of the original controlled reentry vehicle was created through the use of the equations of motion in conjunction with an atmospheric model. A modified linear quadratic regulator alowed the set up of a boundary value problem which specified the Lyapunov exponents and determined the gain matrix as a function of time. The gain matrix can eventually be used in the control system of the vehicle.

14. SUBJECT TERMS

Control, Lyapunov, Atmosphere entry, Chaos, Trajectories

15. NUMBER OF PAGES
101

16. PRICE CODE

17. SECURITY CLASSIFICATION OF REPORT	18. SECURITY CLASSIFICATION OF THIS PAGE	19. SECURITY CLASSIFICATION OF ABSTRACT	20. LIMITATION OF ABSTRACT
Unclassified	Unclassified	Unclassified	UL

GENERAL INSTRUCTIONS FOR COMPLETING SF 298

The Report Documentation Page (RDP) is used in announcing and cataloging reports. It is important that this information be consistent with the rest of the report, particularly the cover and title page. Instructions for filling in each block of the form follow. It is important to *stay within the lines* to meet *optical scanning requirements*.

Block 1. Agency Use Only *(Leave blank)*.

Block 2. Report Date. Full publication date including day, month, and year, if available (e.g. 1 Jan 88). Must cite at least the year.

Block 3. Type of Report and Dates Covered. State whether report is interim, final, etc. If applicable, enter inclusive report dates (e.g. 10 Jun 87 - 30 Jun 88).

Block 4. Title and Subtitle. A title is taken from the part of the report that provides the most meaningful and complete information. When a report is prepared in more than one volume, repeat the primary title, add volume number, and include subtitle for the specific volume. On classified documents enter the title classification in parentheses.

Block 5. Funding Numbers. To include contract and grant numbers; may include program element number(s), project number(s), task number(s), and work unit number(s). Use the following labels:

C	-	Contract	**PR**	- Project
G	-	Grant	**TA**	- Task
PE	-	Program Element	**WU**	- Work Unit Accession No.

Block 6. Author(s). Name(s) of person(s) responsible for writing the report, performing the research, or credited with the content of the report. If editor or compiler, this should follow the name(s).

Block 7. Performing Organization Name(s) and Address(es). Self-explanatory.

Block 8. Performing Organization Report Number. Enter the unique alphanumeric report number(s) assigned by the organization performing the report.

Block 9. Sponsoring/Monitoring Agency Name(s) and Address(es). Self-explanatory.

Block 10. Sponsoring/Monitoring Agency Report Number. *(If known)*

Block 11. Supplementary Notes. Enter information not included elsewhere such as: Prepared in cooperation with...; Trans. of...; To be published in.... When a report is revised, include a statement whether the new report supersedes or supplements the older report.

Block 12a. Distribution/Availability Statement. Denotes public availability or limitations. Cite any availability to the public. Enter additional limitations or special markings in all capitals (e.g. NOFORN, REL, ITAR).

DOD - See DoDD 5230.24, "Distribution Statements on Technical Documents."
DOE - See authorities.
NASA - See Handbook NHB 2200.2.
NTIS - Leave blank.

Block 12b. Distribution Code.

DOD - Leave blank.
DOE - Enter DOE distribution categories from the Standard Distribution for Unclassified Scientific and Technical Reports.
NASA - Leave blank.
NTIS - Leave blank.

Block 13. Abstract. Include a brief *(Maximum 200 words)* factual summary of the most significant information contained in the report.

Block 14. Subject Terms. Keywords or phrases identifying major subjects in the report.

Block 15. Number of Pages. Enter the total number of pages.

Block 16. Price Code. Enter appropriate price code *(NTIS only)*.

Blocks 17. - 19. Security Classifications. Self-explanatory. Enter U.S. Security Classification in accordance with U.S. Security Regulations (i.e., UNCLASSIFIED). If form contains classified information, stamp classification on the top and bottom of the page.

Block 20. Limitation of Abstract. This block must be completed to assign a limitation to the abstract. Enter either UL (unlimited) or SAR (same as report). An entry in this block is necessary if the abstract is to be limited. If blank, the abstract is assumed to be unlimited.